Date: March 31, 2016

To: Black Hills National Forest Service

From: Paul Santi

RE: Executive Summary, Cook Lake Landslide Stability Analysis

Many historic and active landslides surround Cook Lake in the Bear Lodge Mountains located north of Sundance in Crook County, Wyoming. Several slope failures have occurred there within the last 70 years, the most recent of which took place in 1997. This event involved the failure of a 27-acre area on the southwest side of Cook Lake. It is believed that after a two-year period following a record rainfall for Crook County, a subsurface clay unit had become saturated and eventually exceeded its liquid limit, initiating this complex slide. The purpose of this report is to analyze the current stability of the 1997 landslide area by conducting a back-analysis of failure conditions to establish reasonable subsurface material strengths and groundwater levels using a computer simulation model. This analysis is then interpreted to ultimately estimate the probability of landslide reactivation at the site for various groundwater levels. In addition, this report evaluates the runout of the potential future reactivated landslide.

Field observations of the exposed scarp face at the site and the muddy toe near the lake support a conceptual model of the landslide failure plane that follows the paleo scarp deep into the subsurface and then curves to follow the gentle dip of a weak bedding plane. Subsurface material strength ranges used for modeling were based on the results of direct shear tests completed on undisturbed, ground-level samples collected in the field. The direct shear testing results were compared to values published in technical literature sources for similar materials. A constraint on the current location of the water table within the failure area was provided by incorporating locations where ponding and seepage was observed into the working current conditions model.

Results indicate that the northern part of the slide is marginally stable and may move in the future, but that the southern part is less likely to move. The center can be induced to move with high water tables. Future large-scale failures may enter Cook Lake but are not expected to cross the lake. The failure will have the potential to be “rapid” (>3 m/min) (Hunter and Fell, 2003), but combined with runout projections it is not expected to be catastrophic to the campgrounds across the lake.

Summary Report –
Stability Analysis of Cook Lake Landslide
Crook County, Wyoming

March 31, 2016

Prepared for:
Black Hills National Forest Service

Prepared by:
Paul Santi, P.G., Ph.D., Caroline Scheevel, and Emma Bradford
Colorado School of Mines
Department of Geology and Geological Engineering
Golden Colorado 80401

1.0 Introduction

The Cook Lake Recreational Area is located within the Bear Lodge Mountains portion of the Black Hills National Forest, 15 miles north of Sundance, Wyoming (Figure 1).

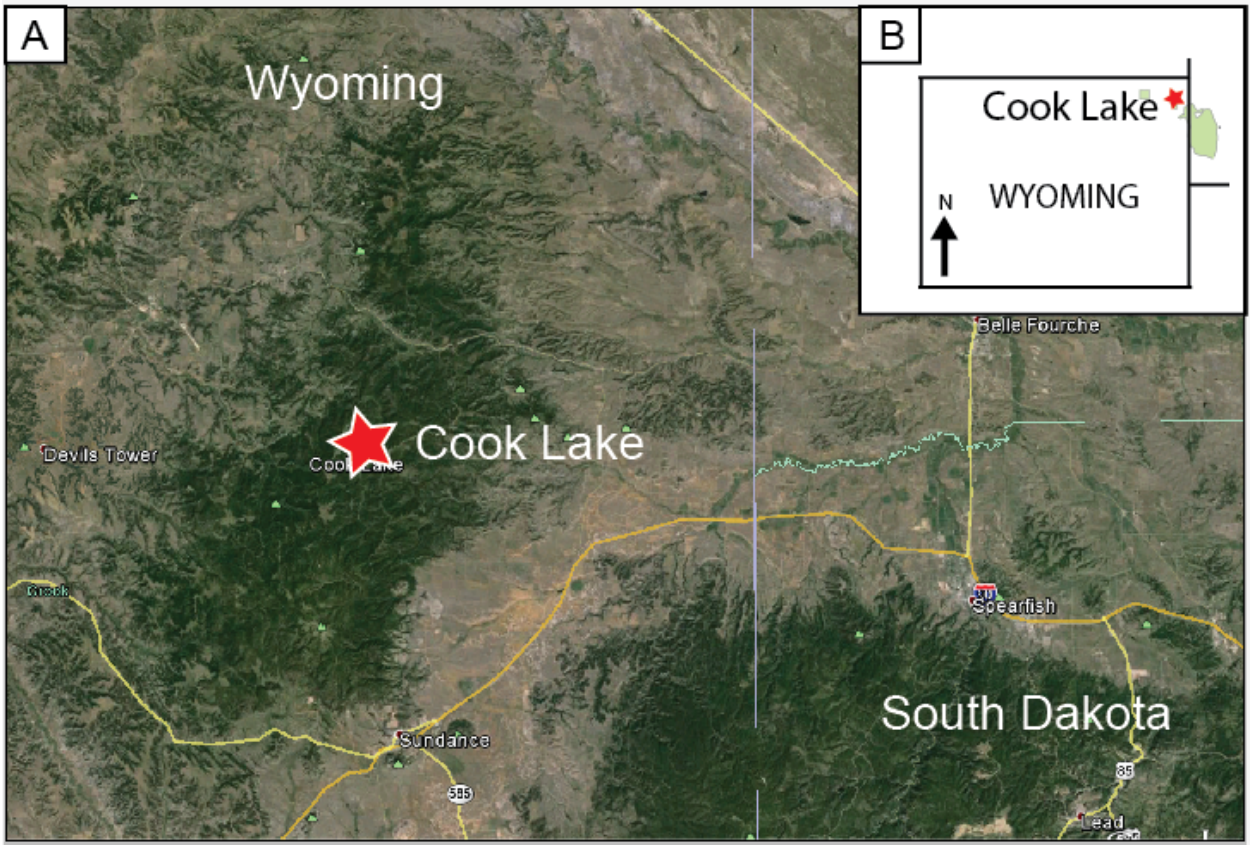

Figure 1. A) Cook Lake is situated north of Sundance, Wyoming and east of Devil's Tower (adapted from Google Earth, 2015). B) The area of interest is in the northeast corner of Wyoming, in the Black Hills National Forest, shown in green.

The area includes thirty-two camping sites, two hiking trails, and a lake formed by the damming of Beaver Creek in the 1940's (Biel, unpublished manuscript, 2014). The recreation area, as well as the surrounding Bear Lodge Mountains, is believed to contain numerous late Quaternary-aged landslide deposits, with a minimum of six active landslides bordering Cook Lake. These have been categorized as multiple block slides with slump components (Wittke, 2011). The most recent regional movement occurred in 1997, when a landslide mobilized along the southwestern edge of the lake overnight (Figure 2). The landslide left a 15 m head scarp and covered approximately 27 acres (Wittke, 2011). In the days following the event, mud volcanoes formed in the lake, which were most likely an extrusion of fluidized clay involved in initiating the sliding process (Karl Emmanuel, personal communication, June 3, 2015). This created what observers referred to as a 'mud island' where the muddy material was extruded from the landslide in such a way that it lies at a higher elevation than surrounding material.

The slide is thought to have interacted with three geologic units (in order from shallowest to deepest): the Cretaceous Lakota Sandstone, the Jurassic Morrison Formation, and the Jurassic Sundance Formation's Redwater Shale Member. The Hulett Sandstone Member underlies the

Redwater Member in the Sundance Formation (Sutherland, 2008). Both the Morrison and the Redwater occur as shales at Cook Lake. All units are relatively flat lying, generally dipping 4°-7° to the northeast.

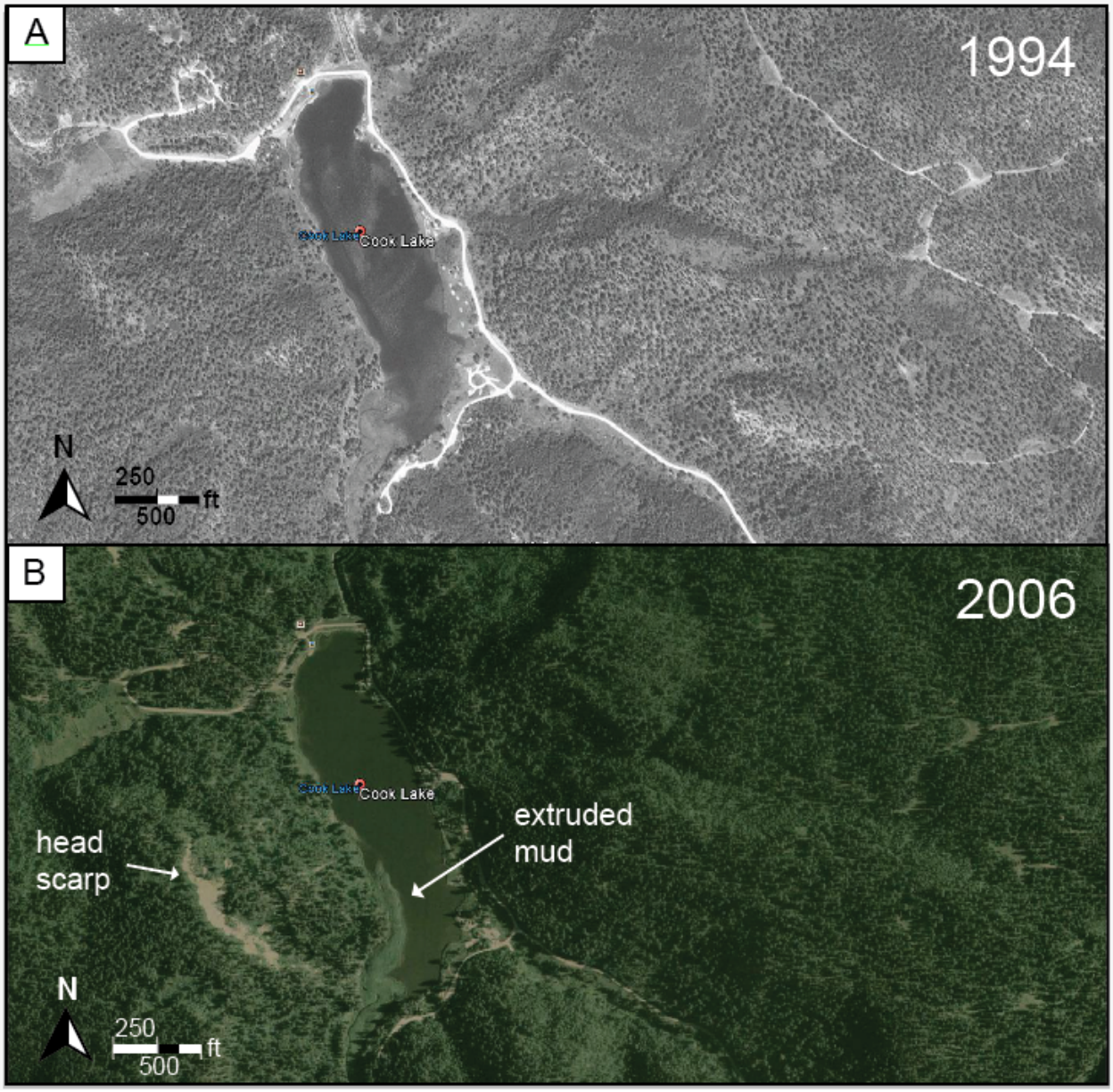

Figure 2. Location of Cook Lake landslide. A) Aerial photo taken of Cook Lake in 1994, prior to failure. B) Aerial photo of Cook Lake in 2006. Note the exposed scarp face and extruded mud toe resulting from 1997 failure. Air photos adapted from GoogleEarth, (2015).

In recent years, the United States Forest Service (USFS) has become concerned that the 1997 landslide could reactivate. The Cook Lake Recreational Area has been temporarily closed since May 9, 2014 after an extremely wet winter and spring. Authorities have been pressed to repair the dam, whose integrity is in question, but do not believe it is prudent to invest funds into

upgrading the dam without knowing the integrity of the site as a whole. A potential landslide reactivation may compromise the area and make it unsafe for pedestrians and unavailable to the public. It is unlikely that additional money will be spent on the dam if the landslide is expected to reactive in a catastrophic manner. This report discusses the stability of the area to the southwest of Cook Lake, the probability that the 1997 landslide will reactivate in the future, and the potential runout distance and velocity of such an event.

2.0 Objectives and Scope of Work

The purpose of the work discussed in this report was to analyze the current and potential future stability of the 1997 landslide region at Cook Lake. Specifically, the following questions were posed:

1. What are the geology, subsurface material strengths, and water conditions at the time of failure based on topography and interpreted landslide geometry before failure in 1997?
2. What geology, subsurface material strengths, and water conditions best represent the slope currently?
3. What is the factor of safety for the slope's current post-failure configuration?
4. What is the expected future stability based on a range of varying groundwater and surface water conditions?
5. What are the risks posed by future movement? If the slide were to reactivate, how long would the expected run-out distance be?

The preceding research questions correspond to four main project tasks:

1. Develop a conceptual model of the area of interest and complete a back-analysis of failure conditions
2. Complete a forward-analysis of current conditions
3. Run a sensitivity analysis of the current slope configuration with respect to varying water conditions
4. Evaluate the risks of a potential future reactivated landslide event in terms of runout distance

The methods, results, and discussion described below are specific to each individual task. Tasks 1 and 2 are discussed in more detail below. Final conclusions and recommendations for potential future work in support of model refinement follow the task sections.

2.1 Conceptual Model Development and Back-Analysis of Failure Conditions

The goal of this task is to develop a conceptual model of the 1997 landslide region immediately preceding the time of failure in terms of geology, subsurface material strengths, and water conditions. An estimation of the failure plane signature is required in order to confirm the consistency of these parameters among three different profiles.

2.2 Conceptual Model Development and Forward Analysis of Failure Conditions

The goal of this task is to develop a conceptual model of future failures using the geology and subsurface material strengths validated in the back-analysis model. The future failure plane is constrained to partially reuse the modeled 1997 failure plane, since that failure plane is expected to be the weakest zone to exploit during a major failure.

3.0 Methods

3.1 Literature Review

The following maps were reviewed:

- Biel, A., unpublished geologic map of Cook lake area, 2015.
- Sutherland, W. M. *Geologic Map of the Devil's Tower 30' x 60' Quadrangle, Crook County, Wyoming, Butte and Lawrence Counties, South Dakota, and Carter County, Montana* [map]. 1:100,000. Laramie, WY: Wyoming State Geological Survey, 2008.
- U.S. Geological Survey. *Black Hills Quadrangle, Crook County, WY* [map]. 1:24,000. 7.5 Minute Series. Reston, VA: United States Department of the Interior, USGS, 2015.
- *USGS NED n45w105 1/3 arc-second 2013 1 x 1 degree ArcGrid.* [computer map]. 1/3 arc-second. The National Map Viewer [website]. Reston, VA: U.S. Geological Survey, 2013. Using ArcGIS [GIS software]. Version 10.3. Redlands, CA: Environmental Systems Research Institute, 1992-2004.

The following documents were reviewed:

- Bergendahl, M. H., Davis, R. E., and Izett, G. A. (1961). "Geology and Mineral Deposits of the Carlile Quadrangle Crook County, Wyoming." *Geological Survey Bulletin,* 1082 – J, 617-655.
- Gesch, D. B. (2007). "The National Elevation Dataset." *Digital Elevation Model Technologies and Applications: The DEM Users Manual,* Maune, D. F., Bethesda, MD :American Society for Photogrammetry and Remote Sensing, 99-118.

- Keefer, W. R., and Love, J. D. (1956). "Landslides along the Gros Ventre River, Teton County, Wyoming." *Wyoming Geological Association (WGA) Eleventh Annual Field Conference*, WGA, WY, 24-28.

- Tighe, M. L., and Chamberlain, D. (2009). "Accuracy comparison of the SRTM, ASTER, NED, NEXTMAP® USA digital terrain model over several USA study sites." *American Society for Photogrammetry and Remote Sensing* (A*SPRS)/Management Association for Prival Photogrammetric Surveyors (MAPPS) 2009 Fall Conference*, ASPRA and MAPPS, San Antonio, TX.

- Wittke, S. J. (2011). "Digital Photogrammetry: An Examination of Automatic Terrain Extraction Methods and Applications." M.S. Thesis, University of Wyoming, Laramie, WY.

3.2 Site Reconnaissance

Approximately ten days of site reconnaissance were performed from June 2, 2015 to June 11, 2015 to observe the current conditions of the slope of interest. After doing a preliminary reconnaissance on June 2nd, Dr. Paul Santi, Emma Bradford, and Caroline Scheevel met with Karl Emmanuel from the Black Hills National Forest Service to discuss the project and visit the site on June 3rd. For the remainder of the time, Emma Bradford and Caroline Scheevel recorded field observations of the 1997 landslide area and other surrounding landslide areas at the Cook Lake Recreational Area. Specifically, the following tasks were performed:

- Recorded comments from Karl Emmanuel regarding potential pre-failure hydrologic conditions and landslide deposit conditions shortly after failure.

- Recorded field observations of geomorphology, hydrology, and geology for the 1997 landslide area, photographing features of interest.

- Delineated three E-W profiles parallel (Fig. 3) to the slide trajectory to closely observe elevations of movement indicators and hydrologic features along each profile.

- Recorded field observations of geomorphology, hydrology, and geology for the other surrounding landslide areas within the recreational area, photographing features of interest.

- Estimated run-out lengths of these landslides based on contextual evidence such as float material roundness, float material lichen growth, and freshness of associated scarps.

- Collected undisturbed surficial samples in the 1997 landslide area of the Morrison Formation, the Redwater Member, and the extruded mud material. Samples were collected by hammering 2.5-inch diameter steel tubes vertically into shallow soil and then excavating and sealing the tubes.

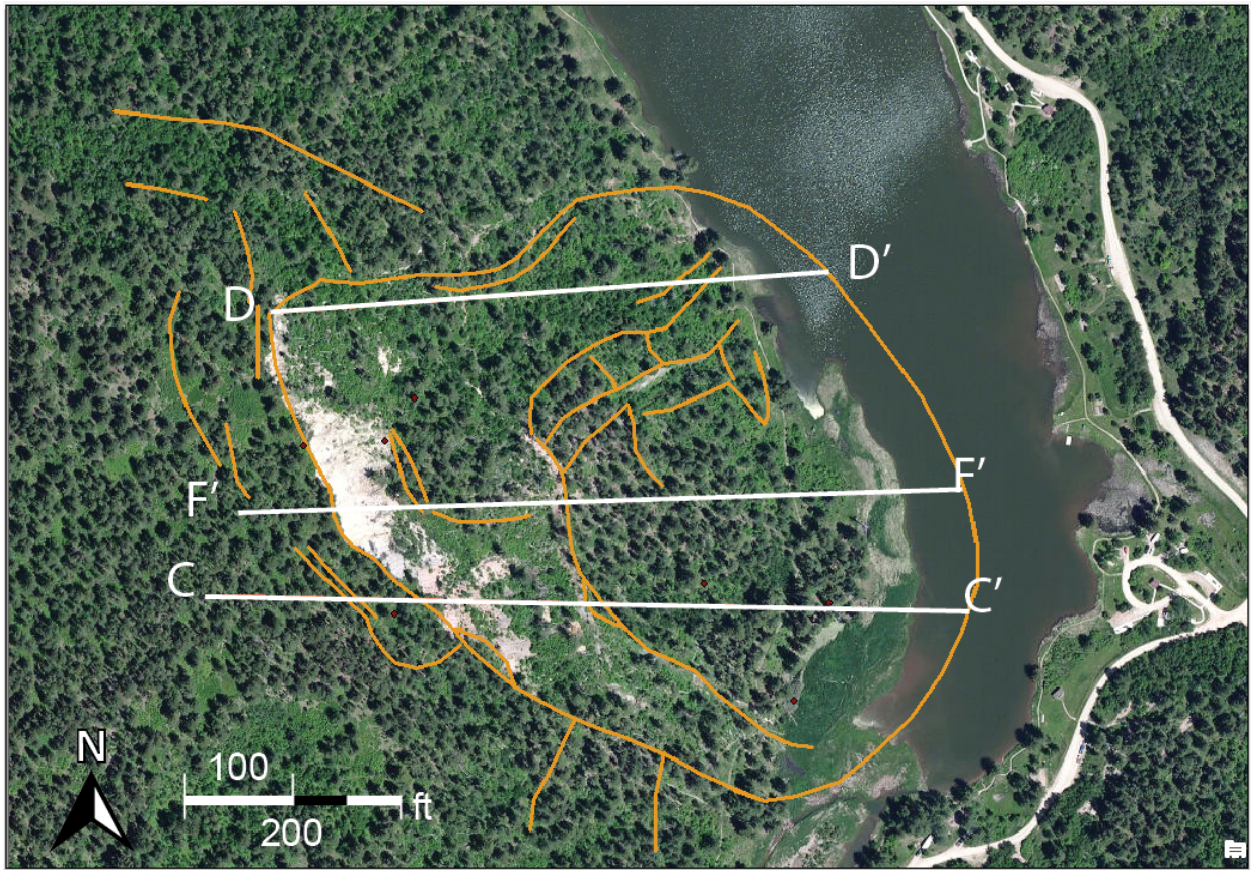

Figure 3. Features emphasized during field reconnaissance. The investigators referenced previous mapping performed by K.M. Emanuel (unpublished internal report, Oct. 29, 2013, shown in orange) and investigated the three east-west profiles, D-D', F-F', and C-C', during site reconnaissance.

3.3 Estimating Material Strength and Density from Field Samples

Direct shear testing was used to develop reasonable material strength ranges. Morrison Formation and Redwater Member samples collected in the field were extruded from the sample tubes and cut to a height of approximately 1.26 in (3.2 cm) in order to obtain a specimen appropriately sized for the direct shear box. Once consolidated under a predetermined weight corresponding to a certain depth below surface, specimens were sheared at a rate of 0.05 in/sec while remaining under the fixed consolidation confining pressure. Shearing was repeated so that residual shear strengths of each specimen could be measured. Full results are included in Appendix A. Material densities were estimated by measuring the mass and calculating the volume of each direct shear test specimen.

Atterberg Limits tests were conducted to find the liquid limit and plasticity index of the Redwater Member and Morrison Formation samples.

Material strength values obtained from direct shear testing and density values were cross-checked with values for similar materials reported in technical literature (Koloski, 1989, "Angle of Friction - Geotechdata.info", 2013, and "Cohesion - Geotechdata.info", 2014). Both material

strength and density value ranges were narrowed by performing a back-analysis of likely failure conditions using the computer program SLIDE 6.0 (Rocscience, 2014) as discussed below.

3.4 Estimating Groundwater Conditions at Failure

Groundwater conditions at the time immediately preceding failure were estimated based on field observations, local geology, and publically available snowpack telemetry (SNOTEL) data of the Bear Lodge Mountains at the Devil's Tower station.

Because the precipitation records do not show anomalously large precipitation events around the time of failure, it was decided that the pre-failure groundwater conditions would be modeled at three generalized levels: high, medium, and low. During site reconnaissance, areas of ponding on the surface of the slope were noted and these locations were used to locate the medium water table, situated within the Morrison Formation. Relative to the placement of the medium water table, the high water table was placed near the contact between the Lakota Formation and the Morrison Formation while the low water table was placed near the contact between the Morrison Formation and the Redwater Member.

3.5 Development of Profiles and Estimated Failures Surfaces for Stability Analysis

The National Elevation Database (NED) was used to create a topographic map of the site and cross-sections for analysis. According to Gesch (2007), the NED is a seamless raster elevation data set that has been compiled from multiple source data sets, all of which have been processed to have the same resolution, coordinate system, elevation units, and horizontal and vertical datums. The NED was created for the first time in 1999 from 7.5 minute digital elevation model (DEM) source data, but since then, some regions have been updated to show improved accuracies based on high-resolution LiDAR or photogrammetric data (Tighe and Chamberlain, 2009). Because there is such a wide breadth of source data sets used to generate the NED, it contains spatial variances in accuracy (Tighe and Chamberlain, 2009). The region corresponding to the Cook Lake Recreational Area on the NED shows identical topographic information when compared to the 1952 Black Hills 7.5 minute quadrangle and therefore represents pre-failure conditions. The USGS considers the Cook Lake Recreational Area to be too small and remote for regular updates of topographic information (Biel, personal communication, 2015).

The pre-failure DEM was acquired from the USGS NED National Map Viewer website, imported into ArcGIS 10.3 (ESRI, 2010), and used to generate a pre-failure hill shade contour map. A series of topographic profiles were extracted from the DEM.

Geologic unit contacts, based on Biel (2015, unpublished geologic map), with corresponding material parameters and estimated groundwater levels were incorporated into the profiles in SLIDE 6.0 (Rocscience, 2014). From this, the failure plane signature was estimated based on field observations and geometry of the local geology. The estimated slide plane was generally oriented parallel to regional dip and drawn with geometry that yielded a factor of safety near 1.0, indicating that the slope was on the verge of failure.

The U.S. Forest Service produced a 1-ft resolution survey of the Cook Lake landslide in October 2015. This post-failure topography DEM was imported into ArcGIS 10.3 (ESRI, 2010) and used to generate a post-failure hill shade contour map. The post-failure topography was extracted along the same east-west profiles and incorporated into the failure models in SLIDE 6.0 (Rocscience, 2014).

The forward failure models confined the major slide plane to the same depth and orientation that was identified in the backward model. The model had the freedom to pick the location of the head scarp and toe for any future failure, but the main sliding plane was kept at the same depth and angle as the 1997 slide because this is a zone of known weakness.

3.6 Predicting Runout Distance

Runout distance and velocity are typically controlled by landslide volume. However, true volume is difficult to calculate for many slides because slide plane depth and geometry are unknown. A proxy volume, V, of

$$V = \text{slide area} \times \text{material thickness at distal edge}$$

is frequently used in estimations (Legros, 2011). Though a truer volume of the Cook Lake landslide can be estimated based on the backward analysis profiles, existing runout models rely on the volume calculations that assume uniform thickness. Uniform thickness is therefore assumed in this analysis.

Area of the Cook Lake slide was calculated in ArcGIS 10.3 (ESRI, 2010) by mapping the slide boundaries on an aerial photograph of the slide. The distal boundary is thought to be submerged beneath the lake, making direct observation of material thickness impractical. Nevertheless, the distal boundary was estimated to have material thickness of 33 ft (10 m). This thickness is thought to be conservative since the deepest point of the slide plane is modeled at 220 feet (67 m) below the pre-failure surface, and shallows towards all margins. The estimated 33 ft distal thickness is less than the likely average thickness, but is considered conservative for the purposes of estimating a runout distance.

Runout is often investigated with respect to the angle of reach, α, which gives the relationship of vertical drop to total horizontal travel (Legros, 2011; Hunger et al., 2005) (Fig. 4). The measurement of angle of reach does not consider the failure mechanism, just the spatial displacement of material. Corominas (1996) identified correlations between α, failure volumes, different failure mechanisms, and slope confinement conditions. Hunter and Fell (2003) verified that these correlations provide a good fit when volume is greater than 10^6 m^3 and less than $1.2x10^{10}$ m^3. The Cook Lake landslide fits these parameters, so this report uses the Corominas (1996) correlations to estimate reasonable angles of reach for different failure modes. Equation 1 estimates α if the landslide reactivates as an unobstructed translational landslide while Equation

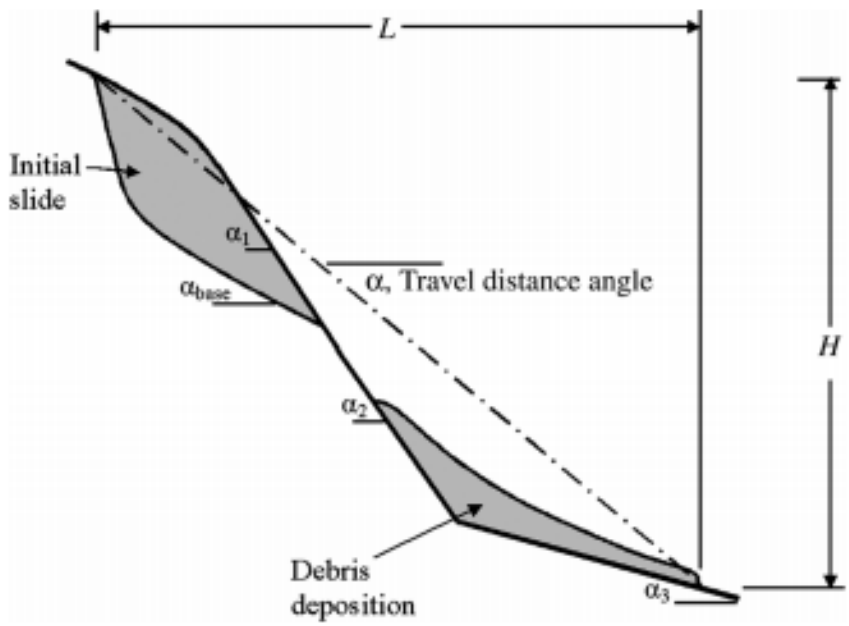

Figure 4. Diagram of angle of reach input parameters. Alpha, noted as travel distance angle, is the tangent of travel height, *H*, to travel distance, *L*. Figure from Hunter and Fell (2003).

2 estimates α resulting from an unobstructed debris flow. Volume is noted as *V* and given in cubic meters (Hunter and Fell, 2003, Corominas, 1996).

$$\log \tan \alpha = -0.143 - 0.080 \log V \quad (1)$$

$$\tan \alpha = 1.028\, V^{-0.1002} \quad (2)$$

The investigators also measured angle of reach of local landslides in the area near Cook Lake. Energy lines, which are the angle of reach projections as seen in map view, were plotted on a landslide site map. The inventory of local angles of reach, correlated with the area covered by the measured slide, was used to validate angle of reach estimates given by Corominas (1996). Projections of all modeled angles of reach were initiated at the same head scarp location identified in the forward model.

Finally, the forward analysis was also used to identify possible runout distances. The model estimates the location of the head scarp and toe of a future failure, but does not indicate how far material might travel past the toe thrust. This would be considered a minimum runout distance.

3.7 Predicting Future Failure Velocity

Rather than specific quantitative values, velocity was evaluated for rapidity, based on the system developed by the International Union of Geological Sciences Working Group on Landslides (IUGS, 1995). Hunter and Fell (2003) refer to “rapid” slides as those with velocity exceeding 10 ft/min (3 m/min), which correlates to the “rapid” (10 ft/min), “very rapid” (16.4 ft/s) and “extremely rapid” (>16. 4 ft/s) classifications noted by IUGS (1995). Soil composition and

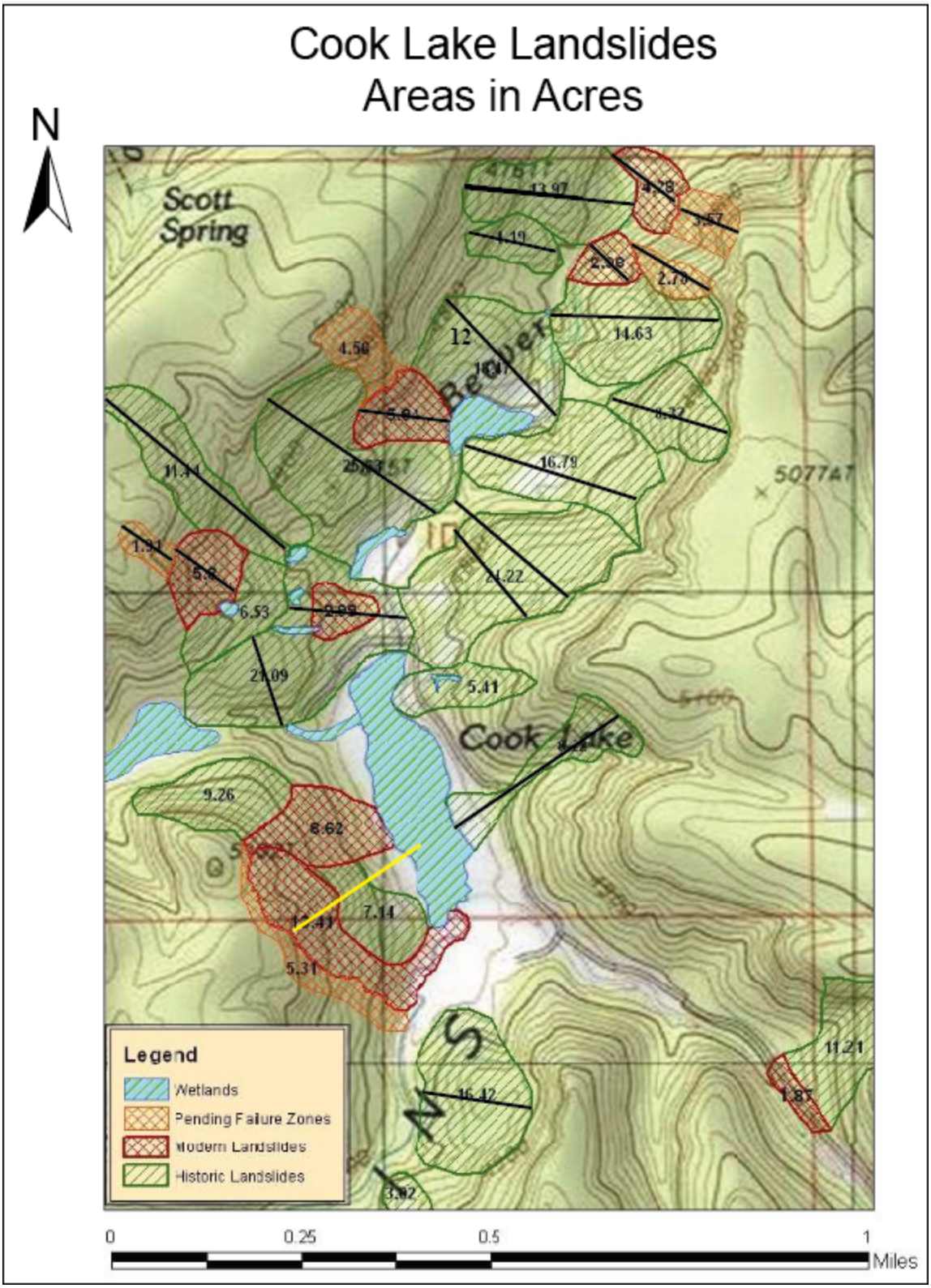

Figure 5. Mapped landslides in Cook Lake area used to inventory local angles of reach. Energy lines were generally oriented perpendicular to topographic lines and along the longest axis parallel to travel. Figure adapted from K.M. Emanuel (unpublished internal report, October 29, 2013).

behavior upon shearing, as discussed in Hunter and Fell (3003) are used to assess the likely failure velocities at Cook Lake.

4.0 Results

4.1 Literature Review

4.1a Regional Landslide Behavior

The geologic map of the Devil's Tower Quadrangle (Sutherland, 2008) indicates that there are three geologic units within the Cook Lake landslide area. These units are Jurassic- and Cretaceous-aged sedimentary rocks described in Table 1. The elevations of the contacts between these units are also shown in Table 1. Based on personal communication with Karl Emmanuel, the units in the area of interest dip gently (approximately 4º - 7º) in a general eastward direction. Both the Morrison Formation and the Redwater Member of the Sundance Formation contain interbedded shale and mudstone layers that are prone to failure (HDR Engineering Inc., 2013; Keefer and Love, 1956).

Table 1. Descriptions of geologic relevant to the 1997 Cook Lake Landslide (adapted from Sutherland (2008)).

Elevation (ft)	Elevation (m)	Unit	Description
5059	1542	Kla	Lakota Formation (Lower Cretaceous) Interfingered and lenticular beds of light-gray to light yellowish-gray claystone, siltstone, and conglomeritic sandstone Maximum thickness of about 300 ft
4918	1499	Jm	Morrison Formation (Upper Jurassic) Light greenish gray to green, pink, and grayish red siltstone and claystone accompanied by thin lenticular light-gray sandstones and shaley limestones Maximum thickness of about 145 ft (44 m)
4723	1440	Jsr	Sundance Formation (Upper and Middle Jurassic) Redwater Shale Member Greenish-gray shale, nonresistant glauconite, interbedded with light-gray, calcareous, fine-grained sandstone, and gray sandy, fossiliferous, oolitic limestone Maximum thickness of 195 ft (59 m)
		Jsh	Sundance Formation (Upper and Middle Jurassic) Hulett Sandstone Member Light grey to light yellowish-gray firmly cemented sandstone Lower 10 to 15 feet frequently contains partings of greenish-gray shale Maximum thickness of 90 ft (27.4)

The Morrison Formation and Redwater Member have failed in several locations across the state of Wyoming, likely due to the very weak shale beds they contain. Many landslides have been identified in areas where these beds dip towards a reservoir or drainage (Keefer and Love, 1956; Bergendahl et al., 1961). In this configuration, edges of the units exposed to water become

saturated while the down-cutting of fluvial bodies undercuts the residual toe material from previous landslides (Figure 4).

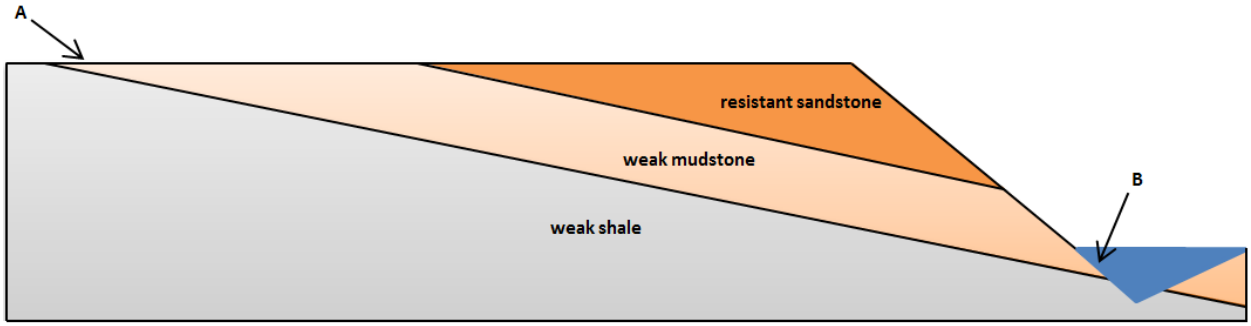

Figure 6. Diagram of failure-inducing water infiltration. Here, 'A' shows an upturned edge of a unit that allows for water infiltration and ultimately saturation. 'B' shows how the down-cutting of the river exposes the base of weak units, prompting a failure surface to form.

This failure mode occurred in the Upper Gros Ventre Landslide, a slow moving landslide that moved from 1908 to 1912 (Keefer and Love, 1956). Another example occurred in the blockslide/slump complex on the north shore of the Keyhole Reservoir, where precipitation was considered a large factor in stability (Bergendahl et al., 1961). Because these units so commonly fail in nearby regions to the site, it is reasonable to assume that the failure plane for the 1997 landslide at Cook Lake cuts through them.

4.1b Material Properties

The Redwater Member and the Morrison Formation are hypothesized to have weathered to the degree that both units exhibited soil-like behavior immediately before and during failure. Atterberg limit testing indicates that the Morrison Formation behaves as a low-plasticity silt (ML) and the Redwater Member as a low-plasticity clay (CL). Literature ranges for materials with the same Universal Soil Classification System (USCS) classification were examined and are summarized in Table 2.

The Lakota Formation, which caps the Morrison Formation and Redwater Member, and the Hulett Sandstone, which underlies the Redwater Member, are hypothesized to have exhibited rock-like behavior before and during failure.

4.2 Field Reconnaissance

4.2a Failure Mode Characteristics

Evidence of rotational failure near the head scarp in the form of uplifted and rotated blocks was noted during reconnaissance (Fig. 7). Blocks closer to the lake do not display rotational signatures. These blocks show pistol-butted trees, indicating regrowth towards vertical after periods of movement and tilting, but do not have pine trees consistently pointing in a single direction.

Table 2. Summary of literature engineering properties related to site geologic units. Walker and Santi (2004) tested the Morrison formation in Colorado. * indicates residual strength

Literature Source	USCS Soil Classification	Associated Geologic Unit	Cohesion (kPa)	Friction angle (degrees)
Geotechdata.info	CL	Redwater	10-20	27-35
	ML-CL	Morrison	~22	27-41
Koloski et al. (1989)	ML	Morrison	0-24	0-35
Walker and Santi (2004)	-	Morrison	41 25*	18 12*

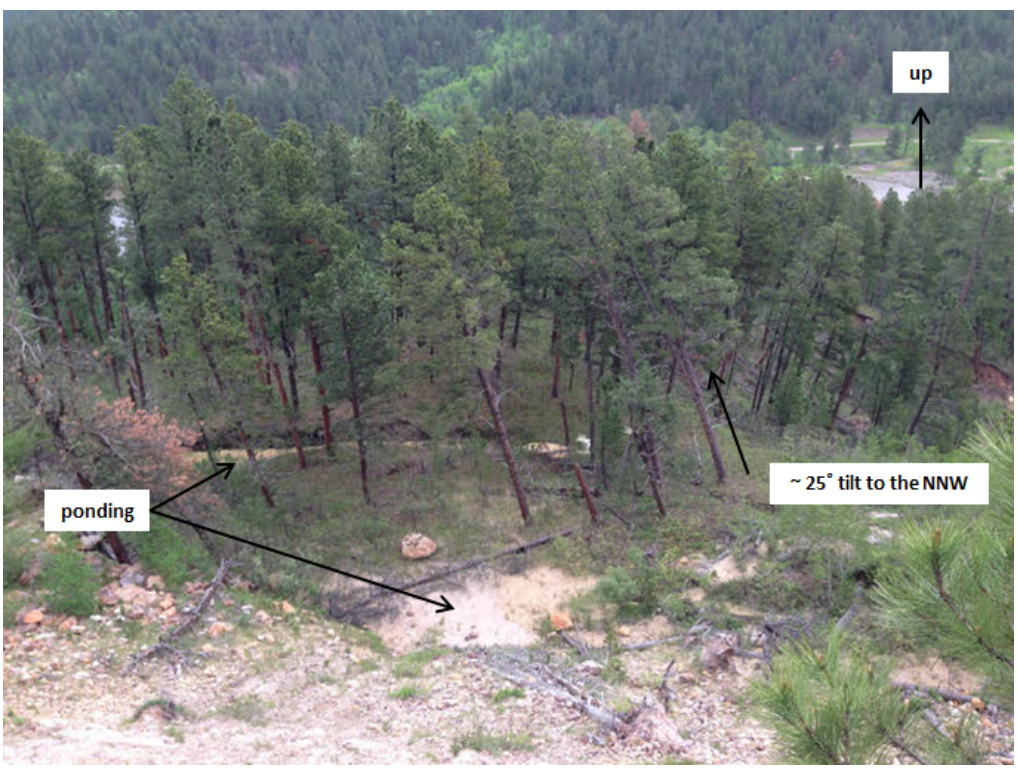

Figure 7. Photograph of rotational features. Northeast-facing photograph was taken from the top of the head scarp. Note that the block below the scarp is bounded by down-dropped blocks (grabens), as indicated by ponding on either side, and rotated, as indicated by the tilted trees. The toe of the slide has thrust upward at the location designated as "up."

The disturbed material at the toe, which formed the initial 'mud islands' was observed on site as bars of soft material exposed at the edge of the lake, visible in Figure 2b. The head scarp was

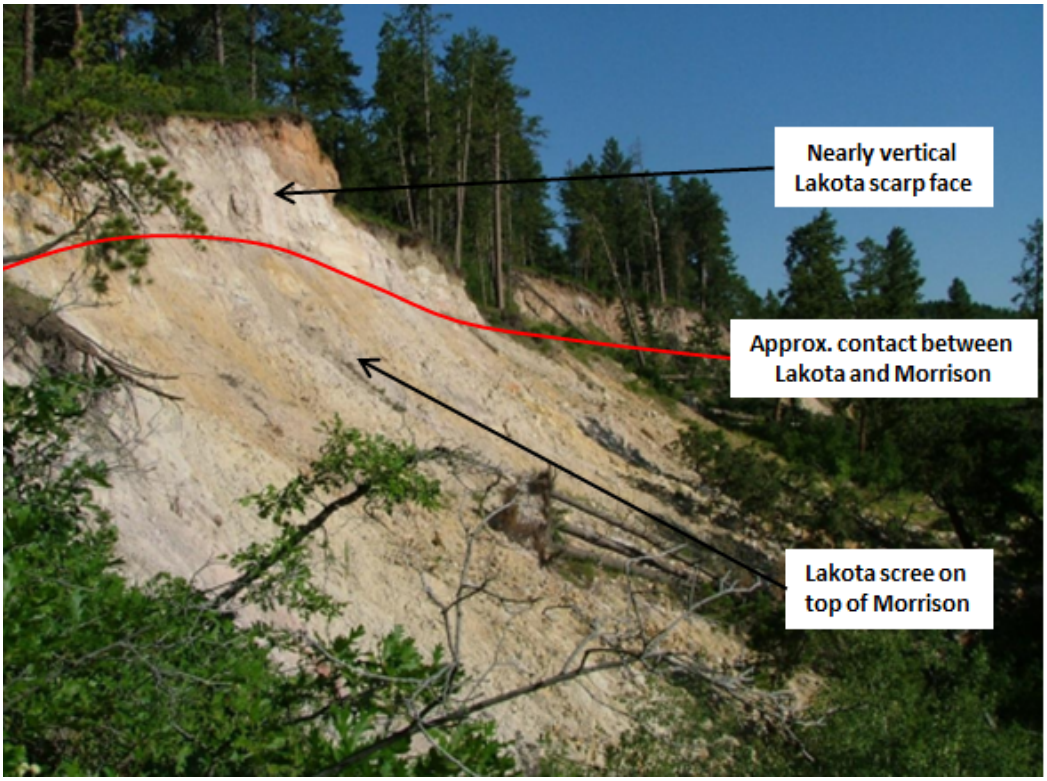

Figure 8. West-facing photograph of the 1997 landslide head scarp where pine trees are approximately 10 m in height (photograph adapted from Wittke (2012).

observed to become increasingly steeper uphill, nearing vertical within the Lakota Formation at the top (Figure 8).

Tension cracks and stream erosion channels were more abundant in the northern part of the slide than in the southern region. Continuous, deep channels filled with phreatophytes were noted near Profile D. Both Profiles D and F were heavily vegetated with areas of steep elevation gain.

Profile C was less vegetated and was located on the edge of a significant graben. The graben contained ponding and the uplifted block shown in Fig. 7, but did not contain any significant stream drainages. No tension cracks were observed near Profile C within the margins of the 1997 slide.

4.2b Material Properties

All three geologic units were observed during site reconnaissance. The Lakota Formation was observed as both a medium-grained tan-colored sandstone as well as a conglomerate. Lakota Formation float material near the scarp was generally boulder-sized with angular to sub-angular roundedness. The Morrison Formation was observed in a variety of colors including maroon, yellow and light teal. When extracting the Morrison Formation from the ground, it was noted that small pebble-sized pieces of material interlocked with one another but immediately crumbled apart upon removal. The Morrison soil was classified as low-plasticity silt (ML). The Redwater Member was generally dark brown and bright red in color. The unit was classified as

low plasticity clay (CL) but there were also clasts of more competent dark yellow sandstone throughout.

A fourth "unit," the disturbed material at the toe, was also sampled. This mud material was organic-rich, completely saturated, and exhibited little to no strength as it could not support the weight of a person walking on top of it. Laboratory tests indicated it was also a low-plasticity silt (ML).

4.2c Groundwater Conditions

Various pooling and seepage of water at the surface was seen throughout the landslide area. Waypoints were taken at these locations and compiled in Table 3.

Table 3. A compilation of UTM coordinates and elevations where pooling or seepage was observed.

Observed Water Locations			
E_UTM	N_UTM	Projected onto Profile:	Elevation (ft)
547045	4937472	C	1451
547022	4937409	-	1446
546963	4937485	C	1470
546762	4937465	C	1514
546702	4937575	F	1538
546755	4937578	F	1531
546774	4937606	F	1527

4.3 Experimental Strength and Density Measurements

All three units were characterized by their unit weight, residual cohesion, and residual friction angle in SLIDE 6.0 (Rocscience, 2014). Table 4 summarizes these residual strength properties, which were obtained from direct shear testing (complete results are available in Appendix A). The disturbed unit data showed substantial variability and did not produce a linear trend when plotted on the normal stress versus shear stress graph; therefore, no values for cohesion or friction angle were calculated and no residual data could be extracted for mud material.

The experimental Morrison friction angle is higher than expected. Walker and Santi (2004) found that the residual friction angle was 11.5° in the Morrison formation in Colorado. The researchers noted small rock fragments in the soil samples which may have affected the results.

The Lakota Formation is primarily hard rock and samples were not amenable for direct shear testing. Its unit weight was the only engineering property that was found experimentally.

Table 4. Averages of experimental direct shear results from residual strength testing.

Unit	Unit Weight (kN/m^3)	Cohesion (kPa)	Friction angle (degrees)
Lakota Formation	21	N/A	N/A
Morrison Formation	19	18	33
Redwater Member	20	28	14
Disturbed Material	13	N/A	N/A

4.4 Back-Analysis of 1997 Failure

4.4a Material Strength Parameters

The experimental values in Table 4 were input into the initial slide models for each profile. Holding the strength parameters constant, the researchers adjusted potential slide planes and possible water tables in search of orientations that yielded factors of safety near 1.0 across all three profiles. No slide plane geometry and consistent water table yielded a satisfactory factor of safety across the three transects. The strength parameters were then iteratively varied by small amounts, attempting to follow trends or remain inside ranges identified in literature (Table 2). The slide plane geometries and water table heights were again also varied until a combination that balanced failure behavior across all three profiles was identified. The final strength parameter inputs are summarized in Table 5. The disturbed material was modeled as a separate geologic unit in the forward models because of its dramatically lower unit weight.

Table 5.Values of Mohr-Coulomb strength parameters used in both backward and forward landslide modeling.

Unit	Unit Weight (kN/m^3)	Saturated Unit Weight (kN/m^3)	Cohesion (kPa)	Friction Angle (degrees)
Lakota Formation	23	24	N/A	N/A
Morrison Formation	17	19	22	33
Redwater Member	19	22	31	16
Disturbed material	13	15	N/A	N/A

4.4b Failure Geometry

The model head scarp in each profile surfaces near the location where modern topography indicates slope movement initiated (Fig. 9). If possible, the scarp is estimated to follow the angle indicated by modern topography until it intersects a dip-parallel plane that can create a toe thrust at the estimated distal boundary. The resulting failure planes are deep seated. The deepest points,

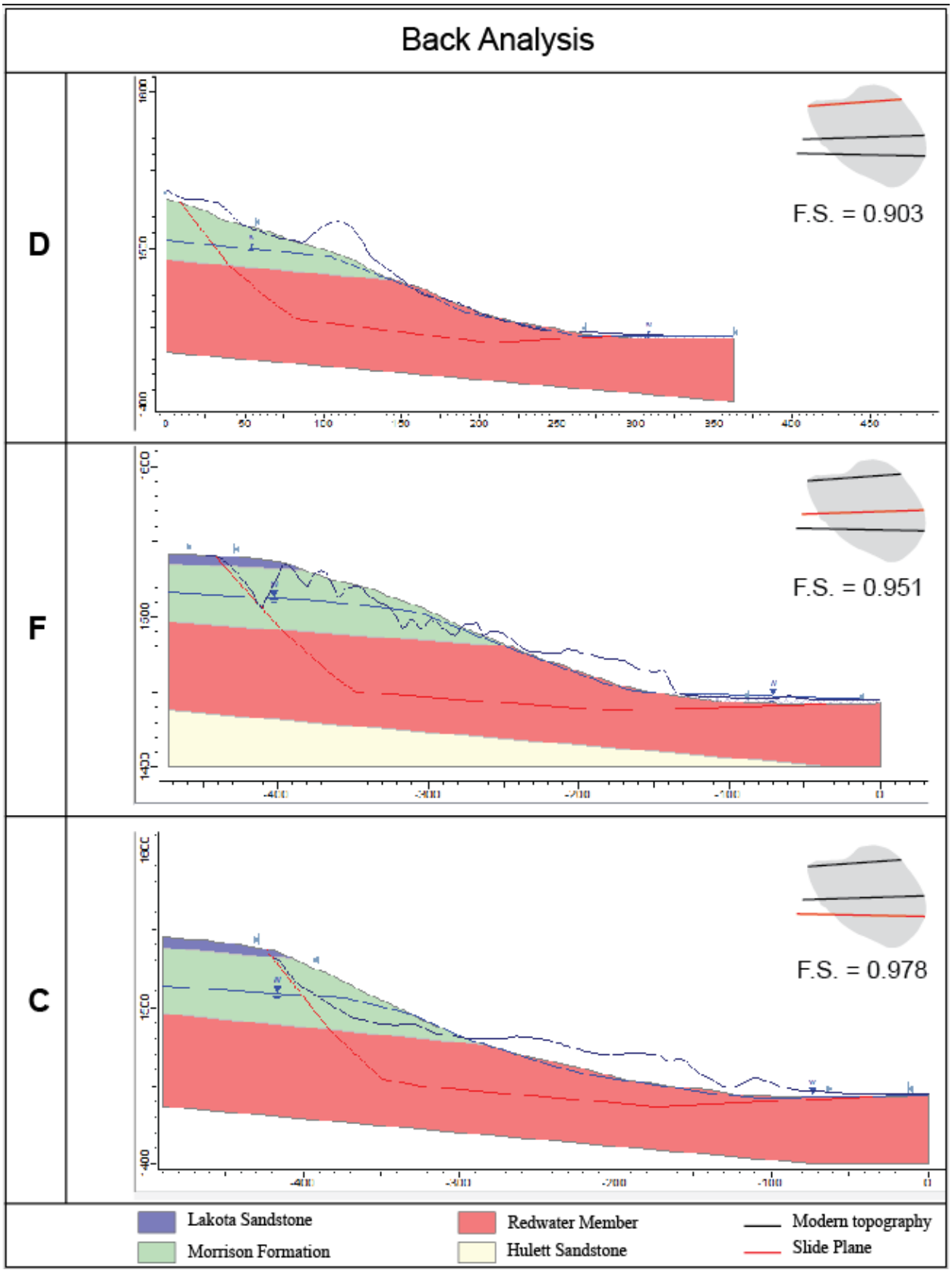

Figure 9. Backward analyzed profiles with medium height water table and 1952 topography. All distances given in meters.

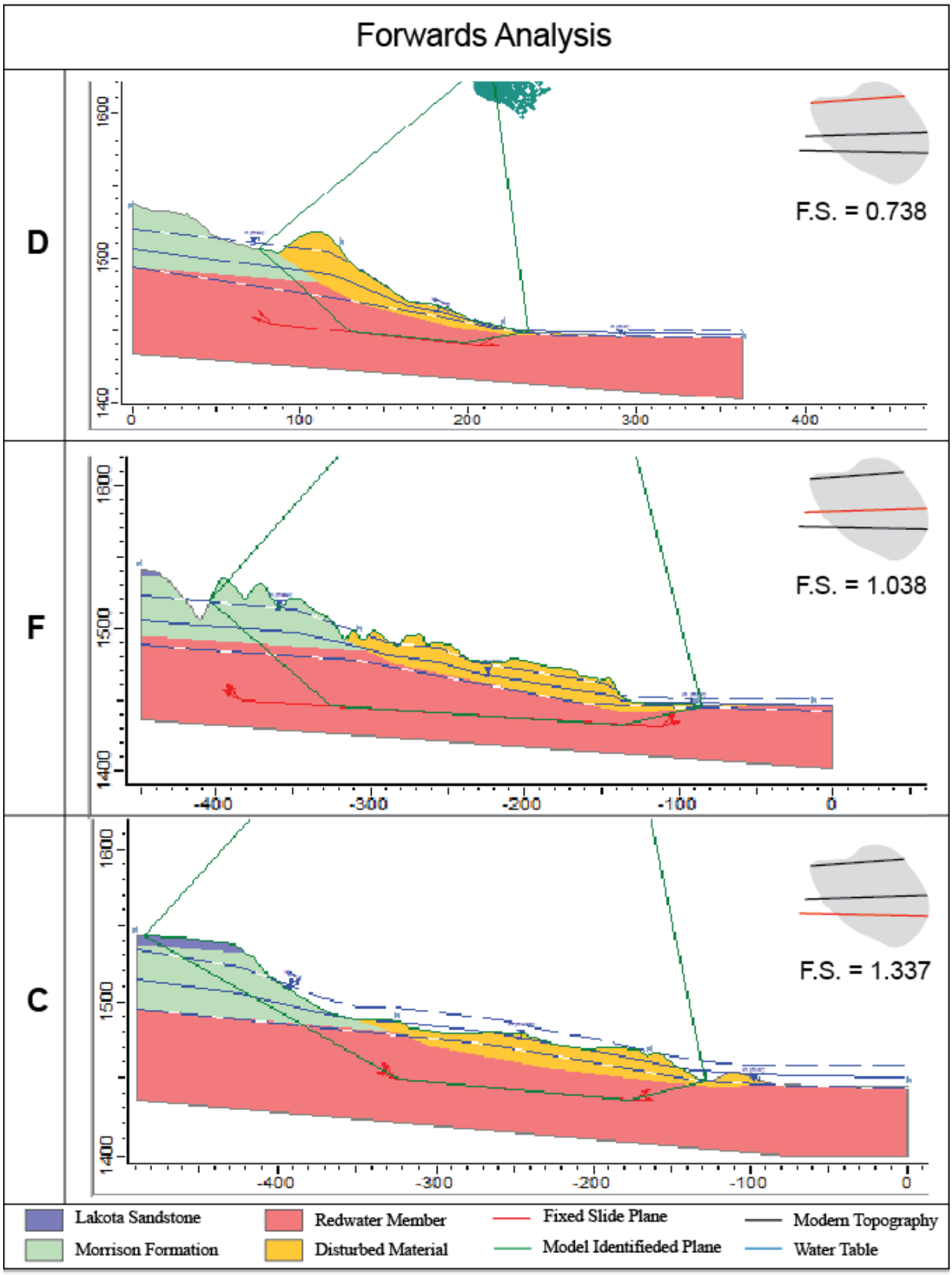

Figure 10. Forward analyzed profiles with all three medium water table heights and 2015 topography. Factors of safety noted are for calculated with the mean, medium water table. All distances given in meters.

from north to south, are 158 ft (48 m), 213 ft (65), and 148 ft (45 m) below ground surface. Shallower geometries do not allow the slide to follow regional dip. This geometry also matches estimates of the shape of the failure surface noted during field reconnaissance. Geometries were adjusted to roughly match across the profiles and yield factors of safety near 1.0.

4.5 Forward Analysis of Future Failure

Disturbed material is drawn to represent the areas of lowered unit weight near the surface, reducing the resisting forces acting at the toe.

The factor of safety increases southward through the slide (Fig. 10). The deepest points along the forward modeled slide planes are shallower than those along the back-modeled slide planes. This occurs because the head scarps enter the slope farther east than the 1997 failure and the toes are located farther west, creating shorter failure zones overall (Fig. 12a). Though the head scarps modeled in Profiles D and F enter the slope at roughly the same east-west location, the toe thrusts do not emerge in line with one another. The modeled head scarp of Profile C is much farther west than the other two profiles and the toe is much farther east (Fig. 12a).

Profiles D and F model smaller volumes of material above the slide plane than were identified in the back-analyzed slide plane. The forward model generally shows the volume of disturbed material increasing progressively to the south. Profile C shows a similar quantity of disturbed material above the slide plane as the quantity disturbed in the back analysis (Figs. 9 and 10).

4.6 Runout Analysis

The angle of reach of the 1997 slide, calculated using 2015 topography, ranges from 14°-19° over the body of the slide. The angles of reach calculated from other slides mapped in the Cook Lake area decrease with increasing area (area is used here as a rough proxy for volume) (Fig. 11). Many slides in the area display $\alpha = 10°$.

Runouts for a future failure are projected in Figure 12 using $\alpha = 10°$, 13°, 14°, and 22° (producing the longest and shortest runouts, respectively). This range was selected to represent the extreme runout ranges measured from nearby landslides (from Fig. 11) and to encompass the potential range calculated for the 1997 slide. The runout modeled in the forward analysis is also shown in Figure 12. All future failure scenarios are assumed to originate at the scarp locations modeled in the forward analysis.

The forward model produces a runout distance similar to the runouts projected using $\alpha = 13°$ and 14°, which is similar to the calculated range of 14°-19°. The longest potential runout, that produced for $\alpha = 10°$, is estimated to extend approximately one-half to two-thirds of the way across the lake. This would not impact campsites or other features near the shore, nor would it impact the dam. Most of the potential runouts would impact the hiking trail that crosses the landslide on the west side of the lake.

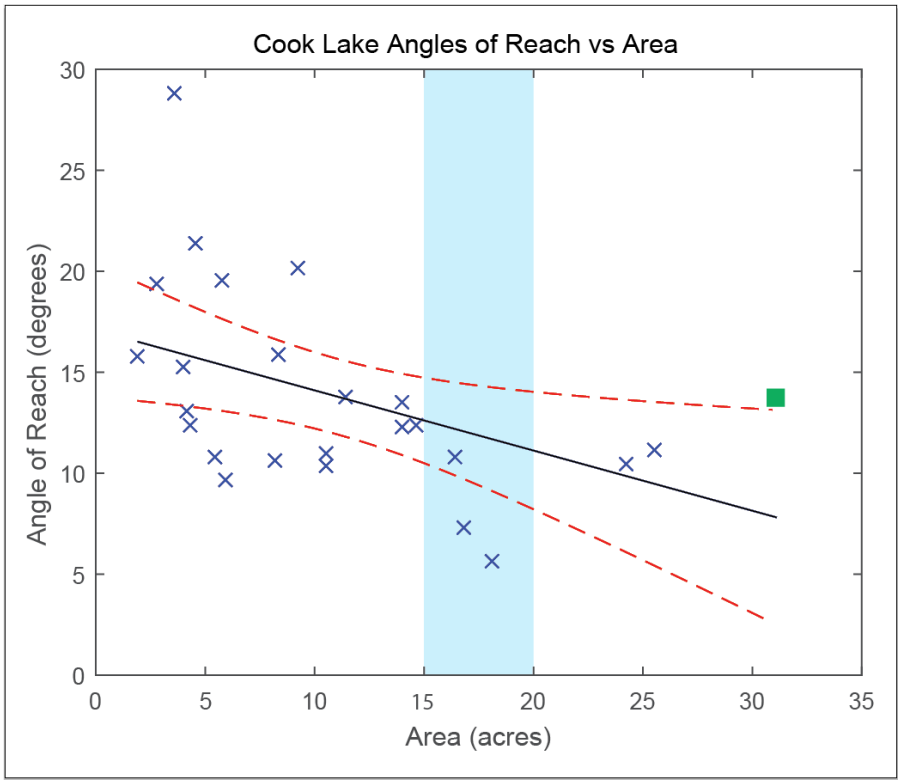

Figure 11. Areas of nearby slides compared to the map-calculated angle of reach. The blue region represents 1/2 - 2/3 of the area disturbed by the 1997 slide, which is assumed to represent the potentially active northern portion of the slide. The black line fits a linear trend to the data. The red dashed lines bound the 95% confidence interval that contains the mean angle of reach for a given area size. The green square indicates measured characteristics of the 1997 slide.

5.0 Discussion

5.1 Literature Review

The regional landslide history suggests that the shear plane for the 1997 Cook Lake landslide is likely in the Redwater Member or Morrison Formation. The Redwater Member was observed in the southern graben (near Profile C), verifying that the slide plane extends into the unit.

The modeled strength parameters do not always fall within the range of the expected literature values. The modeled Redwater Member angle of internal friction (φ), at 16°, is much lower than the range noted in literature, which begins at 27°. This may be because literature sources report values calculated from the peak strength while this report calculated values from the residual strength. If the residual φ is assumed to be 2/3 of the peak φ, the residual angle of friction range would begin at 18° (Walker and Santi, 2004). The modeled residual angle of internal friction is then much closer to the expected value. However, the lower value was selected in order to maintain a conservative approach.

The residual cohesion value for the Redwater Member is also higher than expected, given the values in Table 2. A value of 31 kPa was used in the analysis, although the suggested range in the technical literature was smaller.

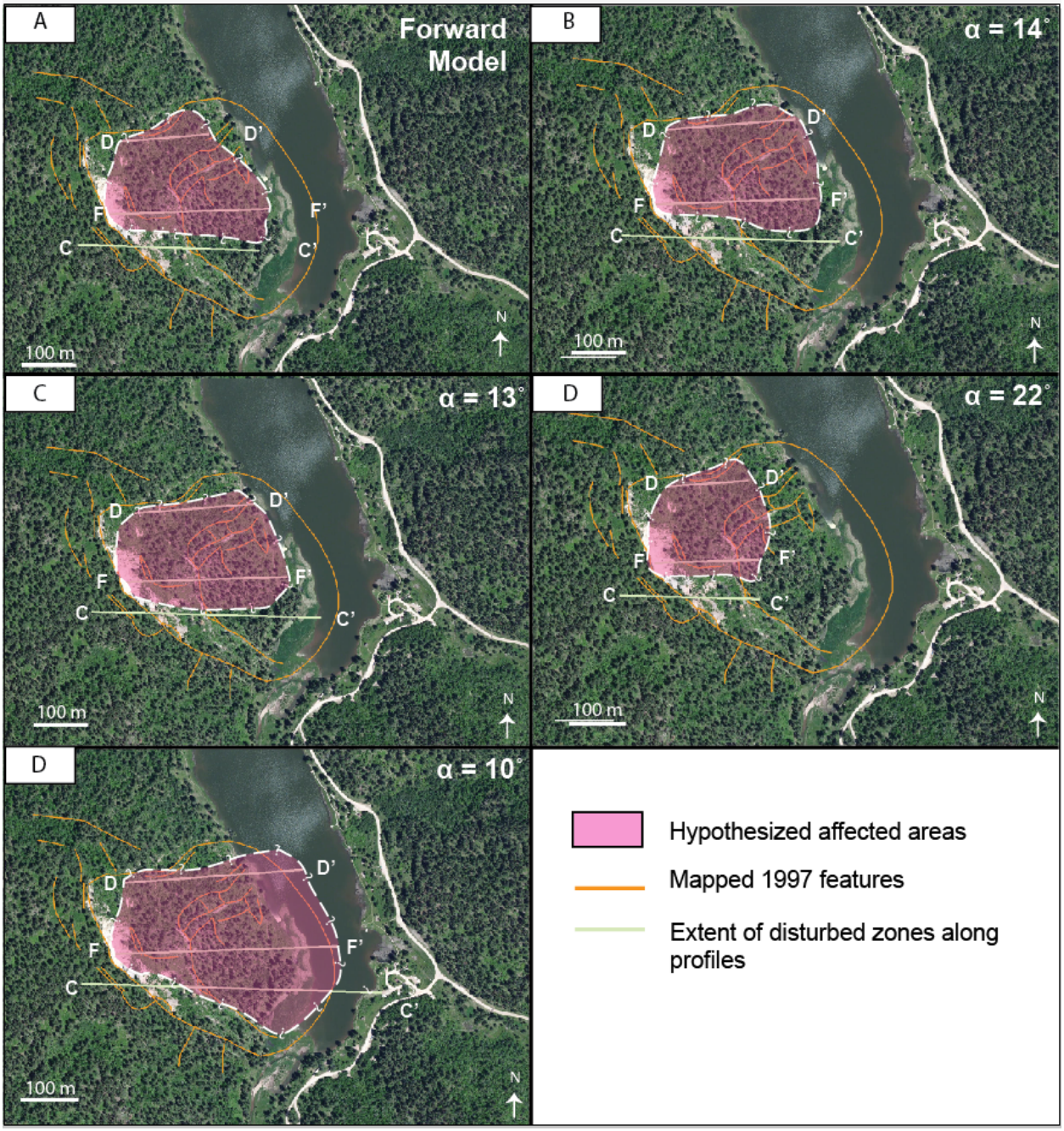

Figure 12. Projected areas disturbed by future slides with angles of reach noted in the subfigures. Note the estimated distal edge in Cook Lake from the 1997 slide, marked in orange. Profile C is not fully included in any hypothesized failure because of its relatively high factor of safety. A) gives the runout directly predicted by the forward model. B-E) Begin the projections at the head scarp location identified in the forward model and then apply the noted angle of reach.

The Morrison angle of friction fits within the expected range of a peak-strength low-plasticity silt. Reduced for residual strength or compared against Walker and Santi (2004), however, the experimental angle is too high. The investigators noted rocky inclusions in the soil, which may have inflated the value. Sensitivity analysis of the model indicates that Morrison φ is not overly

influential on the model stability, so the discrepancy is not expected to have a significant effect (as demonstrated in the sensitivity analysis in Appendix B).

5.2 Field Reconnaissance

The material displacement observed during field reconnaissance indicated both rotational and translational movement. The rotational blocks were more dominant near the scarp, while translational blocks were more dominant near the toe. Consequently, the failure plane is modeled as rotational near the scarp and translational near the toe, with the sliding plane oriented parallel to the regional dip, assuming that a weak bedding plane is exploited.

The presence of a muddy toe thrust block as well as mud volcanoes extruding into the lake only days after failure suggest that there was a significant amount of upward movement near the toe at the time of failure.

These observations, combined with the shallow dip of the bedrock in the direction of sliding and the records of regional failures in both the Morrison Formation and Redwater Member, suggest a failure mode where the failure plane likely extended downward at a steep angle from the scarp in the Lakota Formation. The failure plane then curved in the subsurface near the contact between the Redwater Member and Morrison Formation to follow a shallow dip along an unidentified weak bedding plane. The disturbed mud material at the lake margin is assumed to emanate from a toe thrust west of the location where fluidized mud entered the lake.

5.3 Model Analysis

Several factors limit the accuracy of the slope stability analysis: the 1952 pre-failure topographic map had much lower resolution that the 2015 post-failure map, the elevation of the ground-water table both at the time of failure and currently is unknown, the exact location of the failure plane was estimated, and the strength of materials along the failure plane was extrapolated from samples near the ground surface. Therefore, the absolute values of the calculated factors of safety should not be considered precise. Instead, the relative differences in factors of safety across the different profiles and with changing ground-water conditions should be evaluated to identify sensitive areas (Table 6).

Table 6. Summary of relative changes in factor of safety (F.S.) at each profile. The relative change is more fundamental to understanding the stability at Cook Lake than the absolute factors of safety.

Profile	F.S. Backward Model	F. S. Forward Model	Relative change to F.S.
D	0.903	0.738	- 18%
F	0.951	1.038	+ 9%
C	0.978	1.337	+ 37%

In the backward models, potential failure planes were calibrated to match a factor of safety approximately one for all three profiles. The current site conditions are represented by the forward models. Profile C appears to be more stable in the current configuration, with a calculated increase in factor of safety on the order of 37%. This indicates that the post-failure topography is flatter and lower, as can be seen in Figures 9 and 10. Profile F has roughly the same level of stability post-failure, with a nominal increase in the factor of safety of 9%. Profile D actually shows an increase in likelihood of movement, with a decrease in the factor of safety of approximately 18%. This represents a smaller failure area (see Fig. 9 and 10), and also stems from the unusual uplifted and disturbed zone near the head of the slide. This zone was observed in the field and in the 2015 DEM, but it was difficult to reconcile with the 1952 topography. For this reason, the calculated factors of safety for Profile D are considered conservative and a worst-case scenario. Nevertheless, the post-failure analyses indicate that the southern part of the landslide has increased stability, and the northern part is vulnerable to continued movement.

5.4 Sensitivity Analysis

The described uncertainties in the forward and backward models may mean that modeled factors of safety, even when greater than one, should not be considered exact. Sensitivity plots of the model thus show zones of transition near F.S. = 1, where results of 1.15 and lower may still be considered at risk for stability (Appendix B). Sensitivity analyses of each profile were performed to identify how sensitive the model is to variations in strength parameters. The angle of internal friction, cohesion, and unit weight of each material were varied while holding all other factors at their mean values. Steeper curves indicate that variations in that strength value have more effect on the overall factor of safety than variations along flatter curves.

In the backward sensitivity analysis (Figs. B-1, B-2, and B-3), the Redwater Member displays steep curves across all three profiles and all three parameters. The angle of internal friction is the most influential parameter, followed by unit weight and then cohesion. These results indicate that the Redwater Member controls the stability of the slope and the validity of the model. Future work to refine the model should focus on improving the accuracy of strength and unit weight measurements of the Redwater. The unit weight of the Morrison is also another parameter that exerts strong influence on stability and should be measured with more accuracy.

The sensitivity plots of the strength parameters across the three forward-analyzed transects (Figs. B-4, B-5, and B-6) show similar sensitivity to the three tested parameters as the backward analysis. These figures also illustrate how stability increases southward across the slide. Profile D shows that only strong changes in friction angle result in a stable configuration, but variability in cohesion or unit weight are not enough to produce a high factor of safety. Conversely, Profile C is much more stable across most possible variations in strength and unit weight values.

Sensitivity analysis of the water table height (Fig. 13) shows that while it influences the stability for all three profiles, it only controls movement in the vicinity of Profile F. Profile C is expected to remain stable in all but the most extreme high water table conditions, and Profile D is expected to remain unstable even in the lowest water table conditions.

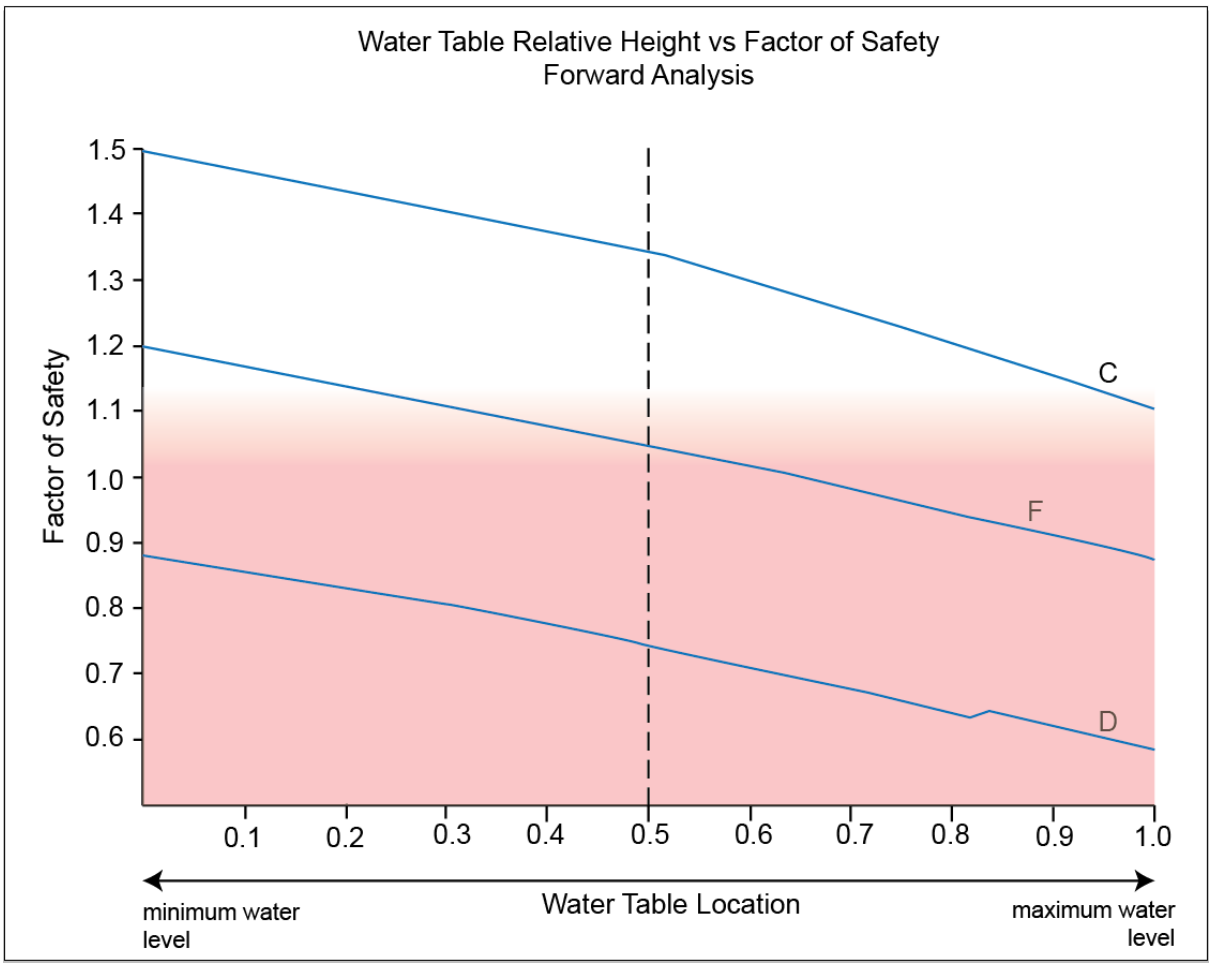

Figure 13. Sensitivity of forward model to changes in the relative water table height. Factor of safety at mean water table level is indicated where profile curves cross the dashed black line. Lowering the water table in Profile D does not stabilize the profile, while raising the water table in Profile C is unlikely to induce failure. Profile F is sensitive to water table height variations.

5.5 Runout Predictions

The forward model estimates the entry and exit points of the slope and toe along each profile (Fig. 12a). Using this model, and assuming that no material flows past the toe boundary, the reactivated material is expected to remain within the margins of the 1997 slide.

Angle of reach projections do not focus on the location of the toe, unlike the forward model. Instead, they estimate the horizontal distance material is expected to move away from the scarp for a given α. Profiles D and F do not show runout that exceeds the boundaries of the 1997 slide when α = 22° (sliding mechanism), 14° (as demonstrated in the 1997 failure), or 13° (unconfined debris flow), even when the full estimated volume of the 1997 slide is mobilized. The full volume is not expected to remobilize since part of the slide near Profile C is expected to be stable. The projections shown in Fig. 12b-d are therefore thought to be conservative estimates of runout for the associated angles of reach.

If the future failure yields α = 10°, as many of the local slides in Figure 3 exhibit, displaced material is expected to enter Cook Lake and push beyond the bounds of the 1997 slide (Fig. 12e). To better evaluate this low α, we examined the relationship between slide area (as a proxy for volume) and angle of reach in Fig. 11. Since full volume of the 1997 slide is unlikely to remobilize, the range of likely α's for the ½ - ⅔ 1997 slide area were examined (Fig. 11). Confidence intervals about the best-fit trend line indicate that α = 10° must still be considered.

Figure 12e shows that material moving along Profile C may travel ½ - ⅔ of the way across Cook Lake when α =10°. The long travel seen along Profile C is a product of the high scarp. If the scarp is lowered because of adjustment related to continued creep along Profile F, the corresponding travel distance *L* will shrink.

5.6 Failure Velocity Predictions

Failure behavior and velocity in soils are largely dependent on whether the soils are contractive or dilative (Hunter and Fell, 2003). Failure velocities generally are slower if a soil has a tendency to dilate upon shearing, rather than contract. Soils are said to be dilative if the pore water pressure at failure decreases and contractive if the pore water pressure increases. Increased pore pressures can cause the effective stress on the soils to drop, allowing movement to occur.

Roughly half of the Redwater Member direct shear tests show the vertical gauge recording upward movement at the time of failure. This implies initial dilative behavior during shearing. The remaining half showed only downward motion, indicating contractive behavior. Dilative behavior was more common at loading pressures representative of shallower depths; specimens tested for pressures at 40 foot depths or deeper showed contractive behavior. Since the forward analysis slide plane is 115–177 ft (35-54 meters) below surface at its deepest point, it is reasonable to think that contractive behavior will occur during the next failure. The direct shear plots of time vs strain show the trend of normally consolidated clays, which are clays that have not previously been exposed to pressures exceeding their current state. Normally consolidated clays are more likely to experience contractive behavior than overconsolidated clays, supporting the hypothesis that the Redwater material will behave contractively.

Atterberg limit tests indicate that the Redwater Shale behaves as a low-plasticity silty clay (CL), while the Morrison Formation behaves as a low-plasticity clayey silt (ML) at Cook Lake. These materials can induce a "flow slide" if the pore water pressure is increased, as it is expected to do when a failure initiates. Flow slides can move rapidly, at the rate of meters per minute (Hunter and Fell, 2003).

Based on these factors, there is a legitimate concern that the reactivated Cook Lake landslide might move rapidly. The slide surface and toe area could be hazardous during wet periods or heavy rainfall or snowmelt.

5.7 Limitations

Because of the limited data available for this analysis, particularly in the subsurface, there are a number of limitations (other than those already mentioned) that affect the accuracy of the analysis.

- The angle of reach is often an underestimate of the true travel distance of a slide (Hungr et al., 2005). The travel distances indicated in Figure 12 should be considered minimums.
- The Redwater Member's ratio of remolded strength to intact strength, known as soil sensitivity, is not known. The risk of a rapid failure is reduced if the sensitivity is low.
- The exact geologic contacts could not be identified in the field; the modeled geologic contacts are not exact.
- The water table in the backward analysis is based on reasonable estimates, but cannot be confirmed. Likewise, the slide plane depth is estimated, and its location as determined by the model may be affected by location of the water table.
- The main basal surface of the modeled slide plane is fixed, but the forward model has the freedom to choose the entry and exit points form the slope. The head scarp may not surface at the exact indicated points because the slope of the plane is steeper in the Morrison than in the Redwater.

6.0 Conclusions

While this type of analysis has limited accuracy without subsurface investigations of material strength, water levels, and identification of the actual failure surface, there are some general slide behaviors that can be anticipated.

- The northern portion of the slide is currently moving.
- The 1997 slide plane is in the range of 145-220 ft (45-67 m) below the ground surface.
- Future failures are likely to exploit the existing weak slide plane.
- Future failures will likely only reactivate a portion of the 1997 slide and involve smaller volumes.
- Four out of five runout projections indicate that the future failure will not mobilize beyond the boundaries of the 1997 slide. The final projection, relying on angles of reach identified at other local Cook Lake landslides, indicates that the slide will enter the lake and exceed the 1997 boundaries. Based on this analysis, it is unlikely that future movement will impact facilities on the east side of the lake.
- The slide may fail rapidly and could create hazards on trails crossing the slide.
- Water table variations have less of an influence at Cook Lake than is typical for landslides. Changed loading conditions, driven by the post-slide topography, are more influential.

7.0 Recommendations for Future Work

A better understanding of the slide movement, potential triggers, and sensitive areas can be developed through additional monitoring and investigation. Some elements might include:

- monitoring of surface survey monuments to track slope movement in real time,
- drilling and installation of piezometers and inclinometers to measure water levels and identify the slope failure surface, respectively, and
- testing of the sensitivity of the Redwater Member, and strength testing of samples from the slide plane.

8.0 References

Angle of Friction – Geotechdata.info. (2013). *Geotechdata.info*. Retrieved 1 August 2015, from http://www.geotechdata.info/parameter/angle-of-friction.html

Bergendahl, M. H., Davis, R. E., and Izett, G. A. (1961). "Geology and Mineral Deposits of the Carlile Quadrangle Crook County, Wyoming." *Geological Survey Bulletin,* 1082 – J, 617-655.

Bieniawski, Z. T. (1989). *Engineering rock mass classifications: a complete manual for engineers and geologists in mining, civil, and petroleum engineering*. New York: Wiley.

Cohesion - Geotechdata.info. (2014). *Geotechdata.info*. Retrieved 1 August 2015, from http://www.geotechdata.info/parameter/cohesion.html

Gesch, D. B. (2007). "The National Elevation Dataset." *Digital Elevation Model Technologies and Applications: The DEM Users Manual,* Maune, D. F., Bethesda, MD :American Society for Photogrammetry and Remote Sensing, 99-118.

HDR Engineering, Inc. (2013). *Rupe Hill Landslide Along US 14*. Retrieved from http://www.dot.state.wy.us/files/live/sites/wydot/files/shared/Environmental_Services/Documents/Rupe%20Hill/Rupe%20Hill%20EA%20FINAL%20June%202013%20wAppendices_web2.pdf

Hungr, O., Corominas, J., & Eberhardt, E. (2005). Estimating landslide motion mechanism, travel distance and velocity. *Landslide Risk Management*, 99-128.

Hunter, G., & Fell, R. (2003). Travel distance angle for" rapid" landslides in constructed and natural soil slopes. *Canadian Geotechnical Journal*, *40*(6), 1123-1141.

IUGS. (1995). A suggested method for describing the rate of movement of a landslide. *Bulletin of the International Association of Engineering Geology*, 52, 75-78.

Keefer, W. R., and Love, J. D. (1956). “Landslides along the Gros Ventre River, Teton County, Wyoming.” *Wyoming Geological Association (WGA) Eleventh Annual Field Conference*, WGA, WY.

Koloski, J. W., Schwarz, S. D., & Tubbs, D. W. (1989). Geotechnical properties of geologic materials. *Engineering geology in Washington*, *1*, 19-24.

Legros, F. (2002). The mobility of long-runout landslides. *Engineering Geology*, *63*(3), 301-331.

Rocscience (2014). "Slide." Version 6.029, Rocscience Inc. 31 Balsam Ave. Toronto, Ontario M4E 1B2, Canada.

Sutherland, W. M. *Geologic Map of the Devil’s Tower 30’ x 60’ Quadrangle, Crook County, Wyoming, Butte and Lawrence Counties, South Dakota, and Carter County, Montana* [map]. 1:100,000. Laramie, WY: Wyoming State Geological Survey, 2008.

Tighe, M. L., and Chamberlain, D. (2009). “Accuracy comparison of the SRTM, ASTER, NED,

NEXTMAP® USA digital terrain model over several USA study sites.” *American Society for Photogrammetry and Remote Sensing* (A*SPRS)/Management Association for Prival Photogrammetric Surveyers (MAPPS) 2009 Fall Conference*, ASPRA and MAPPS, San Antonio, TX.

U.S. Geological Survey. *Black Hills Quadrangle, Crook County, WY* [map]. 1:24,000. 7.5 Minute Series. Reston, VA: United States Department of the Interior, USGS, 2015.

USGS NED n45w105 1/3 arc-second 2013 1 x 1 degree ArcGrid. [computer map]. 1/3 arc-second. The National Map Viewer [website]. Reston, VA: U.S. Geological Survey, 2013. Using ArcGIS [GIS software]. Version 10.3. Redlands, CA: Environmental Systems Research Institute, 1992-2004

Walker, S.R. and Santi, P.M. (2004). Influence of the Blue Mesa Reservoir on the Red Creek Landslide, Colorado. *Environmental And Engineering Geoscience*, *10*(1), 13-26. http://dx.doi.org/10.2113/10.1.13

Wittke, S. J. (2011). “Digital Photogrammetry: An Examination of Automatic Terrain Extraction Methods and Applications.” M.S. Thesis, University of Wyoming, Laramie, WY.

Appendix A – Results of Laboratory Testing

Table A-1. All measured Morrison Formation residuals strengths. Normal stress is calculated using depth and the individual density of the sample. Data are plotted in Figure A-1.

All Morrison Residuals		
Depth (ft)	**Normal Stress, σ (kPa)**	**Shear Stress, τ (kPa)**
5.5	30.49	48.27
11	60.99	67.67
12	60.99	53.40
17	91.48	65.99
22	121.98	102.36
21	121.98	95.98
31	182.97	132.20
36	213.47	161.58
42	243.95	162.05
45	274.45	197.48
51	304.94	226.39
59	365.93	267.42

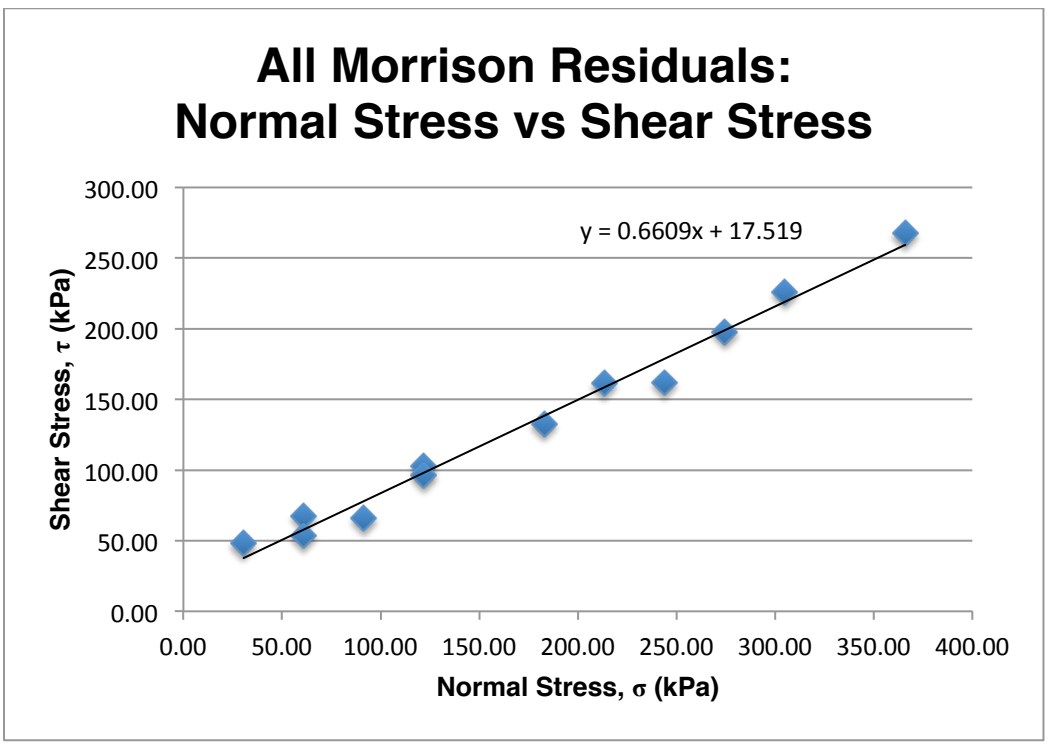

Figure A-1. The Morrison residuals follow a linear trend of the form $\boldsymbol{\tau = c + \sigma * \tan\ \varphi}$, where c is cohesion and φ is the internal angle of friction. The experimental cohesion and internal angle of friction are determined from this plot and summarized in Table A-3.

Table A-2. All measured Redwater Formation residuals strengths. Normal stress is calculated using depth and the individual density of the sample. Note that Sample 1c is much denser than the others. Data are plotted in Figure A-2.

All Redwater Residuals				
Sample No.	**Initial Density (kg/m^3)**	**Depth (ft)**	**Normal Stress (kPa)**	**Shear Stress (kPa)**
2	1716	6	30.49	46.41
1a	1818	6	30.49	29.62
1a	1818	10	60.99	42.68
1c	1932	10.55	60.99	65.99
2	1716	12	60.99	48.27
1b	1768	12	60.99	34.57
2	1716	18	91.48	52.94
1a	1818	19	121.98	58.53
1b	1768	23	121.98	53.87
1c	1932	30.25	213.37	97.70
2	1716	36	182.97	86.23
1b	1768	39	243.95	94.44
1a	1818	41	335.44	102.36
1b	1768	53	335.44	121.95
1c	1932	59.7	426.93	153.47
1c	1932	82.7	609.89	175.29

Table A-3. Experimental results for cohesion and internal angle of friction of both Morrison Formation and Redwater Member.

Unit	Samples Included	Cohesion, c (kPa)	Internal Angle of Friction, φ (°)
Morrison	All samples	17.5	33.2
Redwater	1a, 1b, 2	28.3	14.5
	1a, 1b, 1c, 2	32.3	14.1

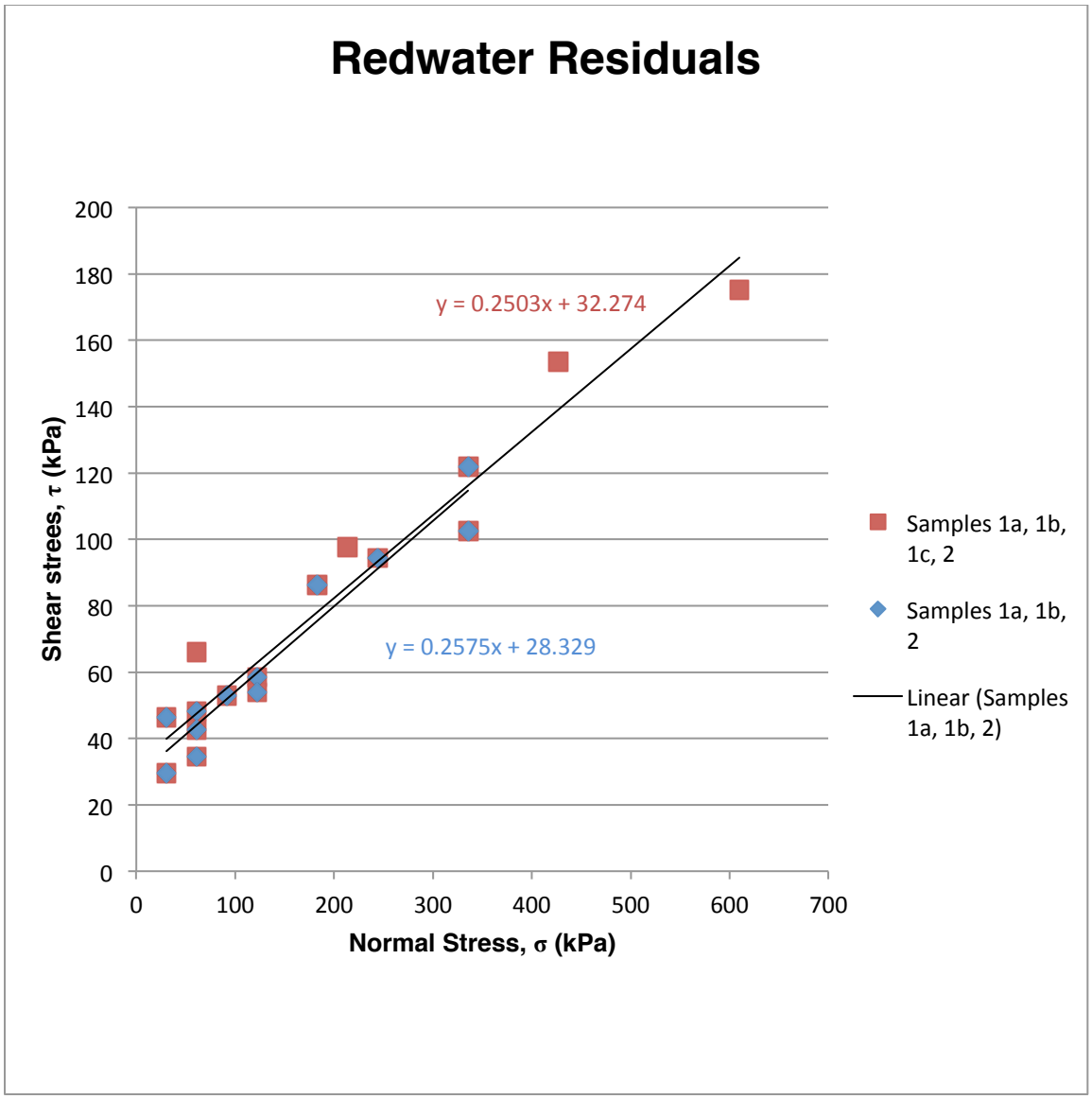

Figure A-2. Sample 1c was denser than the other three samples, so data were examined both with and without Sample 1c. Cohesion, c, and internal angle of friction, φ, are determined using the linear trend and the Mohr-Coulomb relationship $\boldsymbol{\tau = c + \sigma * tan\varphi}$.

Appendix B – Results of Sensitivity Analysis

Table B-1. Ranges used for sensitivity analysis of backward model. These ranges apply to figures B-1 trough B-3.

Backward Sensitivity Analysis Values				
Unit	Property	Mean	Rel. Min.	Rel. Max.
Lakota	Unit Weight	23	20	32
Morrison	Cohesion	22	10	34
	Phi	33	12	41
	Unit Weight	17	15	21
Redwater	Cohesion	31	10	35
	Phi	16	10	30
	Unit Weight	19	15	23

Table B-2. Ranges used for sensitivity analysis of forward model. These ranges apply to figures B-4 through B-6.

Forward Sensitivity Analysis Values				
Unit	Property	Mean	Rel. Min.	Rel. Max.
Lakota	Unit Weight	23	20	32
Morrison	Cohesion	22	10	34
	Phi	33	12	41
	Unit Weight	17	15	21
Redwater	Cohesion	31	10	35
	Phi	16	10	30
	Unit Weight	19	15	23
Disturbed Material	Cohesion	10	1	10
	Phi	35	25	45
	Unit Weight	13	10	22

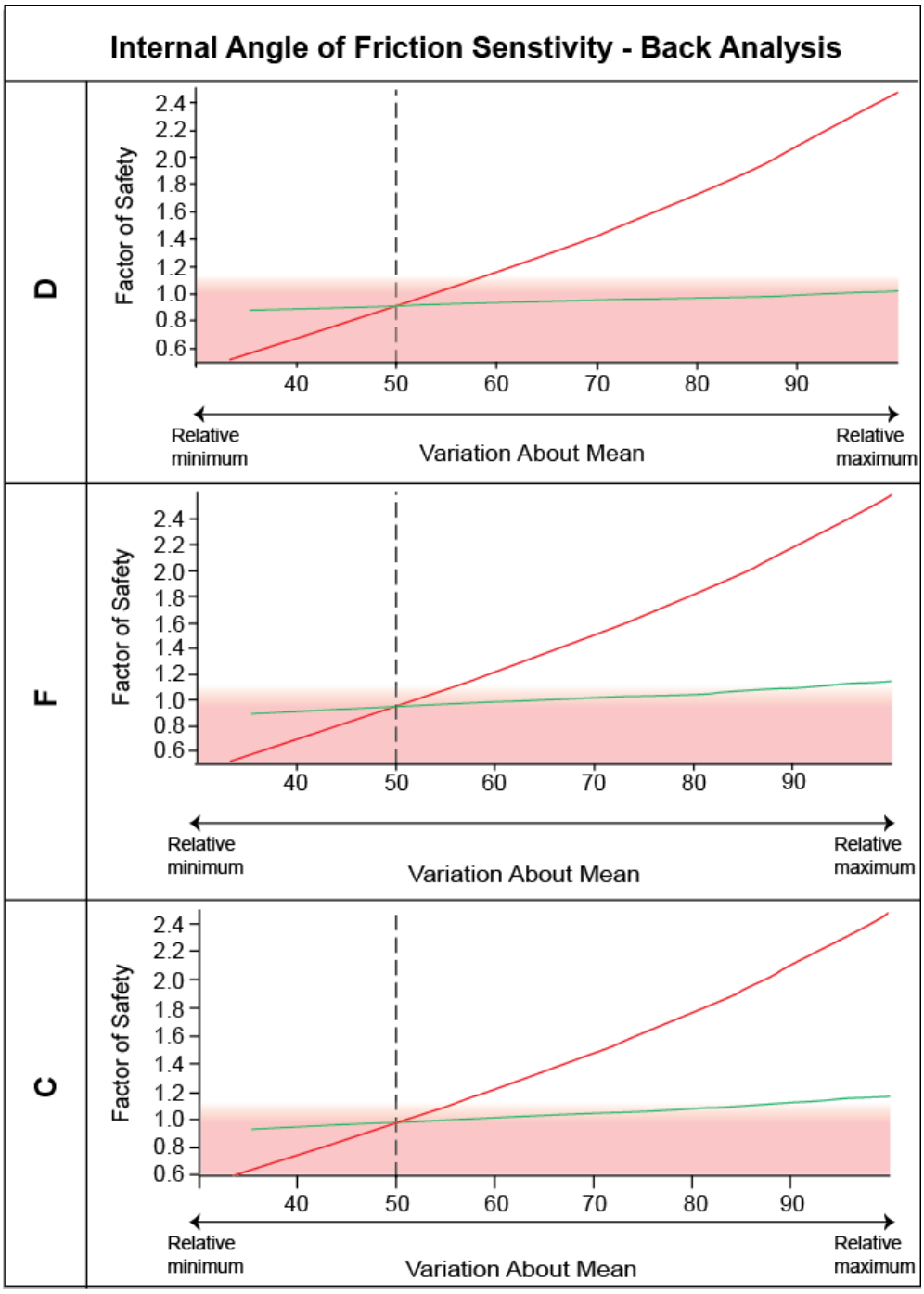

Figure 14. Backward model sensitivity to variation in angle of internal friction. The mean angle of friction for each geologic unit occurs at 50%, indicated with a dashed black line. The red Redwater curve is steep and crosses into the region below F.S. = 1.0, indicating that variations in Redwater friction angle strongly influence the stability of the model. The green Morrison curve remains relatively flat and variations in its strength have minimal influence on the stability of the model. The pink gradational region indicates the range of factors of safety that may lead to failure. The region extends above F.S. = 1.0 to account for inaccuracies in the model.

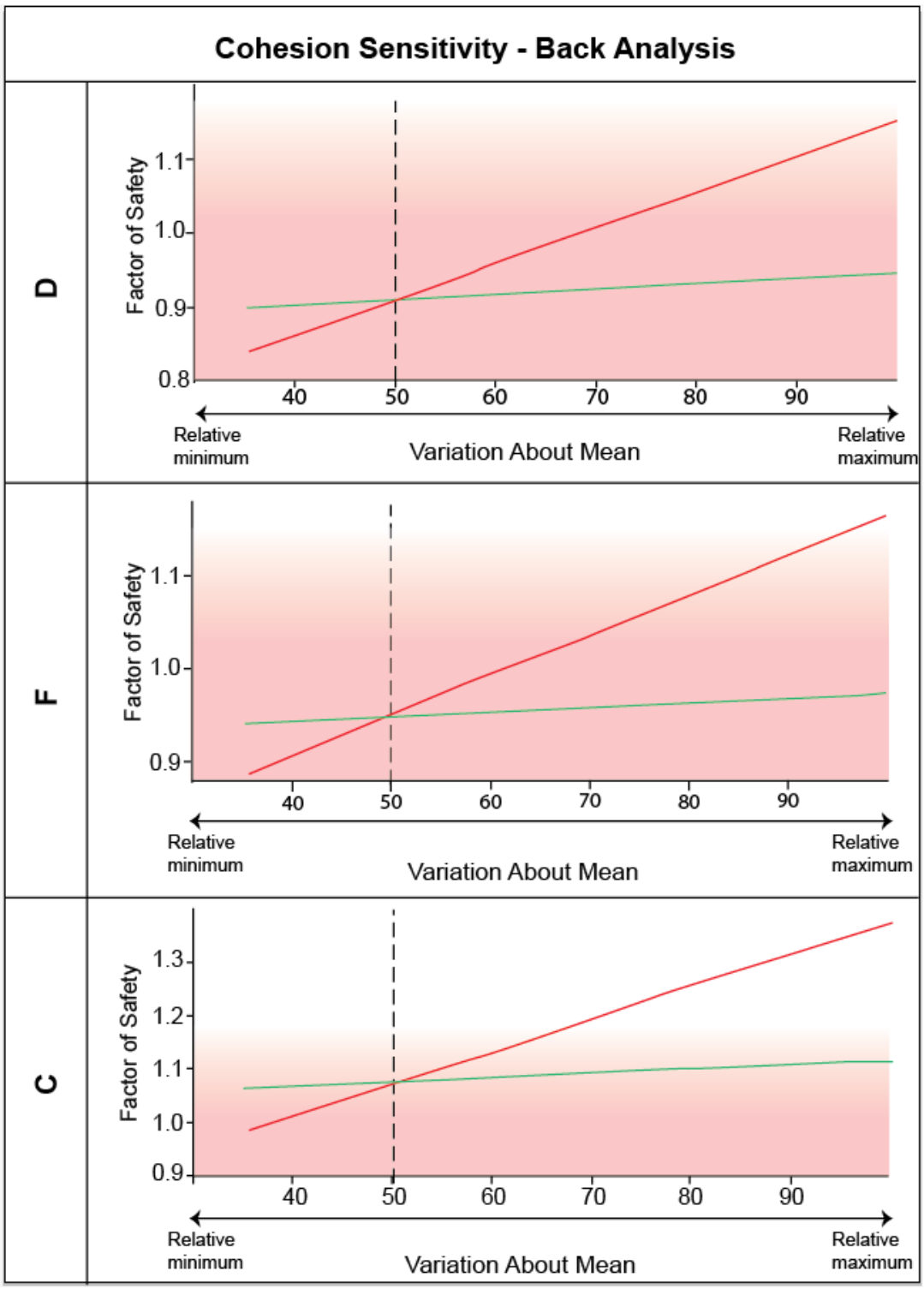

Figure B-2. Backward model sensitivity to variations in cohesion. The mean cohesion for each geologic unit occurs at 50%, indicated with a dashed black line. While variation in cohesion does affect stability, it does not exert near the influence as friction angle. The red Redwater curve is steep and has the strongest influence on stability. The green Morrison curve is relatively flat and exerts minimal influence on the stability. The pink gradational region indicates the range of factors of safety that may lead to failure. The region extends above F.S. = 1.0 to account for inaccuracies in the model.

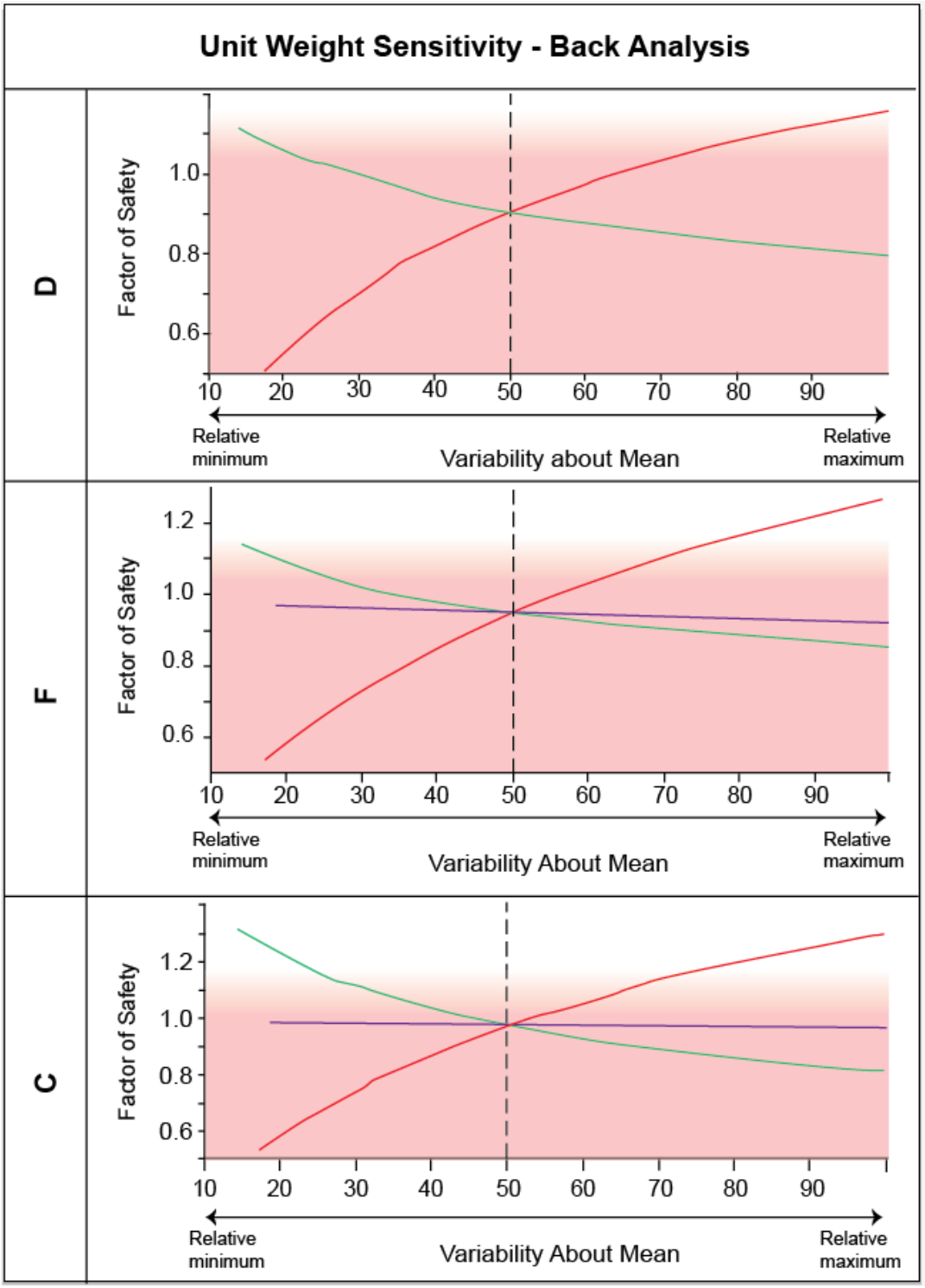

Figure B-3. Backward model sensitivity to variation in unit weight. The mean unit weight for each geologic unit occurs at 50%, indicated with a dashed black line. The purple curve indicates Lakota, the green curve indicates Morrison, and the red curve indicates Redwater. Variations in the unit weight of the Morrison and Redwater have strong influence on slope stability, but variations in the Lakota do not. The pink gradational region indicates the range of factors of safety that may lead to failure. The region extends above F.S. = 1.0 to account for inaccuracies in the model.

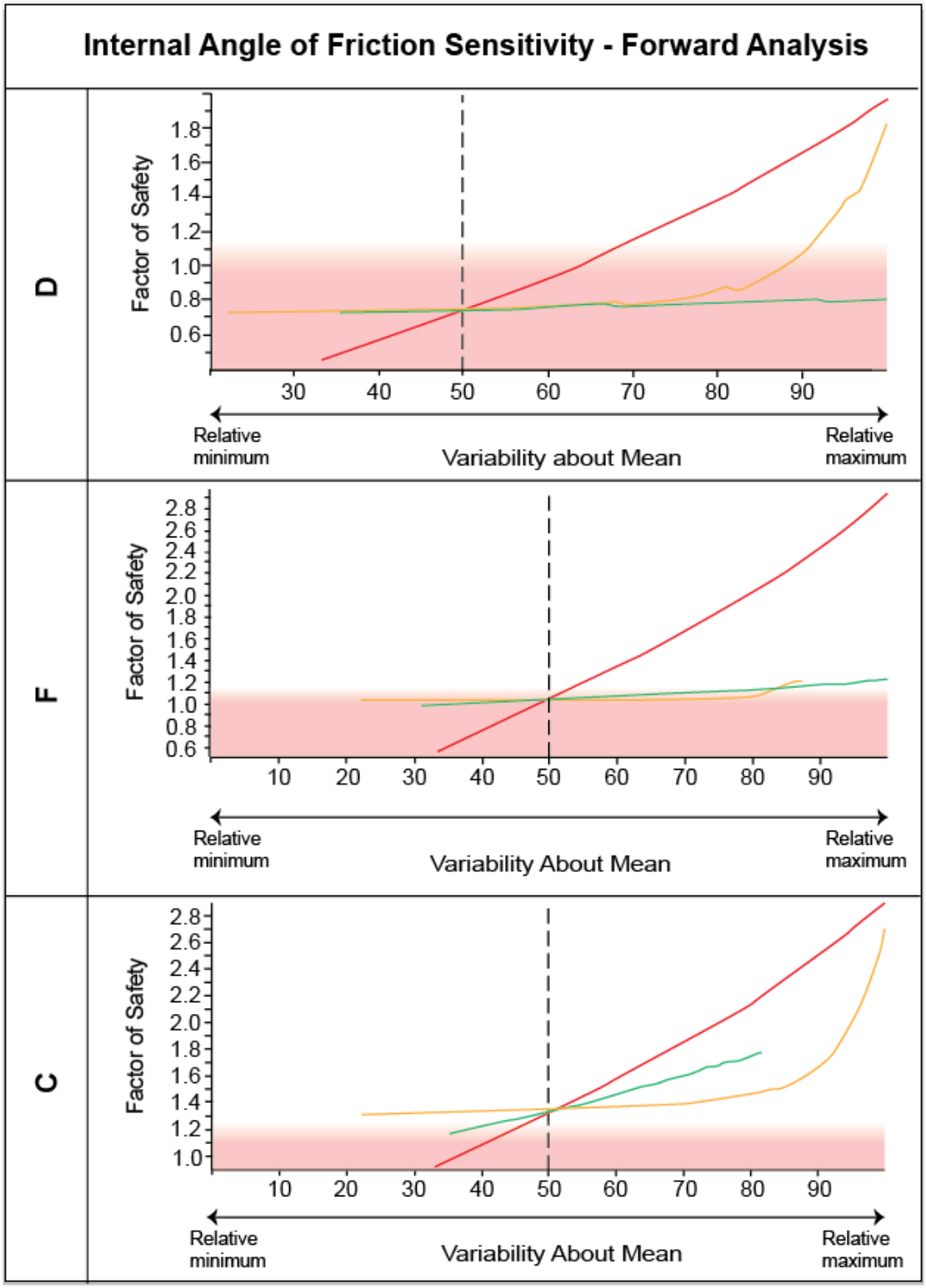

Figure B-4. Forward model sensitivity to variation in angle of internal friction. The mean angle of friction for each geologic unit occurs at 50%, indicated with a dashed black line. The green curve indicates Morrison, the red curve indicates Redwater, and the orange curve indicates the disturbed material. The red Redwater curve is steep and variations in Redwater friction angle strongly influence the stability of the model. The pink gradational region indicates the range of factors of safety that may lead to failure. The region extends above F.S. = 1.0 to account for inaccuracies in the model.

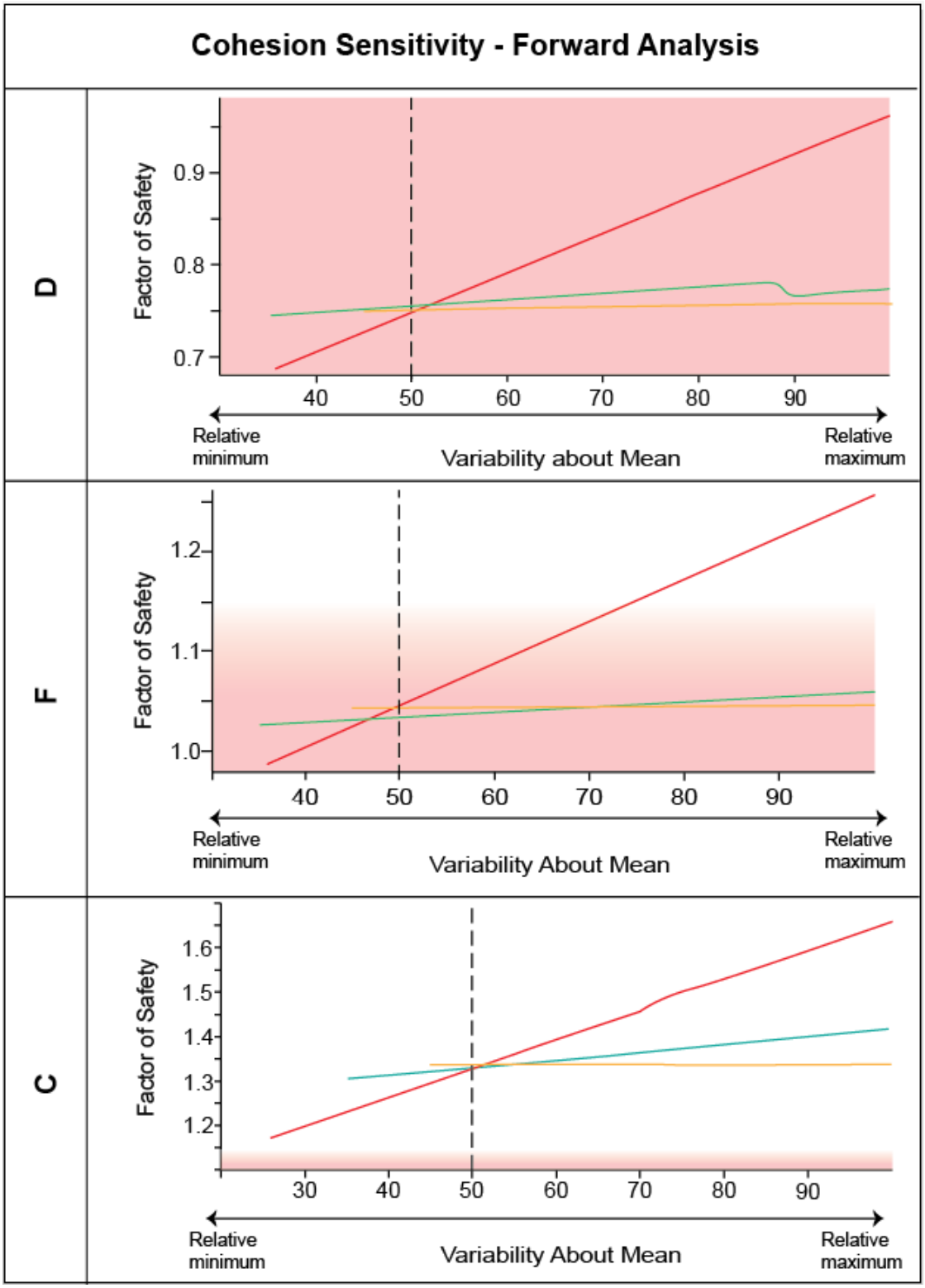

Figure B-5. Forward model sensitivity to variation in cohesion. The mean cohesion for each geologic unit occurs at 50%, indicated with a dashed black line. The green curve indicates Morrison, the red curve indicates Redwater, and the orange curve indicates the disturbed material. The red Redwater curve is steep and variations in Redwater friction angle strongly influence the stability of the model. The pink gradational region indicates the range of factors of safety that may lead to failure. The region extends above F.S. = 1.0 to account for inaccuracies in the model.

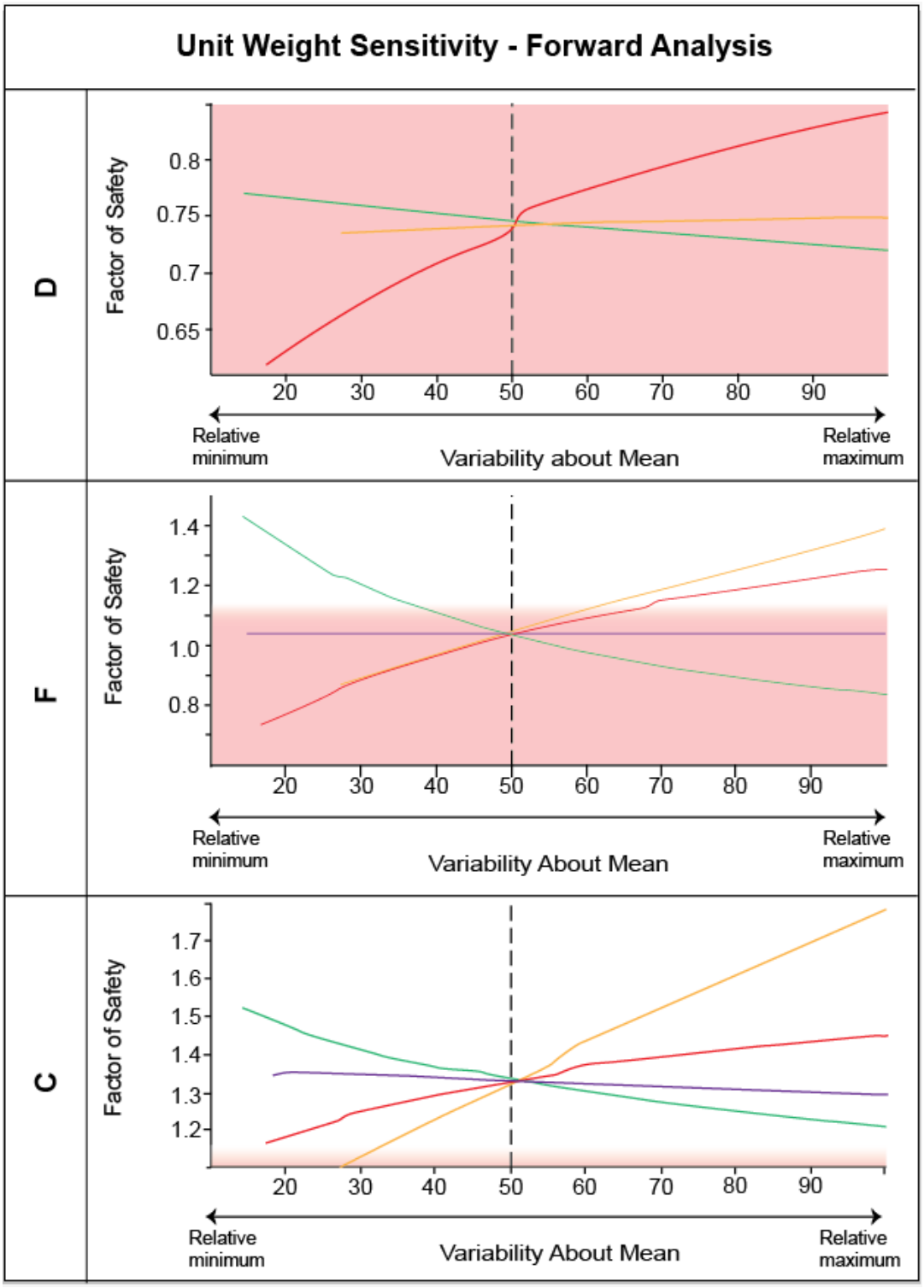

Figure B-6. Forward model sensitivity to variation in unit weight. The mean unit weight for each geologic unit occurs at 50%, indicated with a dashed black line. The purple curve indicates Lakota, the green curve indicates Morrison, the red curve indicates Redwater, and the orange curve indicates the disturbed material. All units except Lakota demonstrate some influence on the stability of the model. The pink gradational region indicates the range of factors of safety that may lead to failure. The region extends above F.S. = 1.0 to account for inaccuracies in the model.